Plant Cell Advance Publication. Published on October 1, 2019, doi:10.1105/tpc.19.00272

RESEARCH ARTICLE

A GDSL Esterase/Lipase Catalyzes the Esterification of Lutein in Bread Wheat

Jacinta L. Watkins[a,h], Ming Li[b,h,i], Ryan P. McQuinn[a], Kai Xun Chan[c,d] , Heather E. McFarlane[e,j], Maria Ermakova[f], Robert T Furbank[f], Daryl Mares[b], Chongmei Dong[g], Kenneth J. Chalmers[b], Peter Sharp[g], Diane E. Mather[b,k] and Barry J. Pogson[a,k]

[a] Australian Research Council Centre of Excellence in Plant Energy Biology, Research School of Biology, Australian National University, Canberra, Australian Capital Territory 0200, Australia

[b] School of Agriculture, Food and Wine, The University of Adelaide, Waite Campus, Glen Osmond, South Australia 5064, Australia

[c] Ghent University, Dept. of Plant Biotechnology and Bioinformatics, Technologiepark 71, 9052 Ghent, Belgium

[d] VIB Center for Plant Systems Biology, Technologiepark 71, 9052 Ghent, Belgium

[e] School of Biosciences, The University of Melbourne, Melbourne, VIC 3010, Australia

[f] Australian Research Council Centre of Excellence in Translational Photosynthesis, Research School of Biology, Australian National University, Canberra, Australian Capital Territory 0200, Australia

[g] Plant Breeding Institute and Sydney Institute of Agriculture, The University of Sydney, 107 Cobbitty Road, Cobbitty, NSW 2570, Australia

[h] These authors contributed equally to this work.

[i] Current address: Wheat Quality Breeding, Institute of Crop Sciences, Chinese Academy of Agricultural Sciences, 12 Zhongguancun South Street, Haidian District, Beijing, 100081

[j] Current address: Department of Cell and Systems Biology, University of Toronto, 25 Harbord St, Toronto, ON, M5S 3G5, Canada

[k] Corresponding authors: Barry Pogson (barry.pogson@anu.edu.au) and Diane Mather (diane.mather@adelaide.edu.au).

Short title: Carotenoid esterification in wheat

One-sentence summary: The discovery of an apoplastic enzyme responsible for esterifying carotenoids that is unexpectedly spatially-separated from its plastidic substrate, lutein, affords new ways to biofortify crops.

The authors responsible for distribution of materials integral to the findings presented in this article in accordance with the policy described in the Instructions for Authors (www.plantcell.org) are: Barry J Pogson (barry.pogson@anu.edu.au) and Diane Mather (diane.mather@adelaide.edu.au).

ABSTRACT

Xanthophylls are a class of carotenoids that are important micronutrients for humans. They are often found esterified with fatty acids in fruits, vegetables and certain grains, including bread wheat (*Triticum aestivum*). Esterification promotes the sequestration and accumulation of carotenoids, thereby enhancing stability, particularly in tissues such as in harvested wheat grain. Here, we report on a plant xanthophyll acyltransferase (XAT) that is both necessary and sufficient for xanthophyll esterification in bread wheat grain. XAT contains a canonical Gly-Asp-Ser-Leu (GDSL) motif and is encoded by a member of the GDSL esterase/lipase (GELP) gene family. Genetic evidence from allelic variants of wheat and transgenic rice calli demonstrated that XAT catalyzes the formation of xanthophyll esters. XAT has broad substrate specificity and can esterify lutein, β-cryptoxanthin and zeaxanthin using multiple acyl-donors, yet it has a preference for triacylglycerides, indicating that the enzyme acts via transesterification. A conserved amino acid, Ser-37, is required for activity. Despite xanthophylls being synthesized in plastids, XAT accumulated in the apoplast. Based on analysis of substrate preferences and xanthophyll ester formation in vitro and in vivo using xanthophyll-accumulating rice callus, we propose that disintegration of the cellular structure during wheat grain desiccation facilitates access to lutein promoting transesterification.

INTRODUCTION

Carotenoids are lipid-soluble pigments produced by photosynthetic organisms, yet they accumulate across all kingdoms of life. They are responsible for many of the bright red, orange and yellow colors of fruits and flowers. The C_{40} polyene backbone provides the pigments with their chromophore. Modifications such as cyclization, addition of oxygen-containing functional groups or changes in conjugation give rise to over 1100 different naturally-occurring carotenoids (Yabuzaki, 2017). In plants, carotenoids have many functions, including acting as accessory light-harvesting pigments, protecting the photosynthetic apparatus from reactive oxygen species produced during stress, and providing precursors for the production of phytohormones. Several carotenoids, including β-carotene and β-cryptoxanthin, provide provitamin A activity that is required for human development, immune function and visual health. Non-provitamin-A carotenoids, such as lutein and zeaxanthin, are also important for human nutrition. High intake of these carotenoids correlates with a lower risk of developing chronic degenerative diseases such as age-related macular degeneration, diabetes, obesity, cardiovascular diseases and certain types of cancers (Tapiero et al., 2004; Concepcion et al., 2018; Kijlstra et al., 2012; Tanaka et al., 2012). Recently, lutein has also been found to be important for cognition during all stages of life (Giordano and Quadro, 2018; Johnson, 2014). Because humans and animals cannot synthesize carotenoids de novo, dietary intake is essential for human health. While fruits and leafy vegetables are the main sources of carotenoids in the human diet, over half of humanity's global caloric energy intake is provided by three nutritionally poor cereals: wheat, rice and maize. Enhancing the biosynthesis and/or preventing degradation of carotenoids in any of these crops could provide an opportunity to improve the nutritional status and health of at-risk populations around the globe.

The carotenoid biosynthesis pathway leading to lutein and its regulatory mechanisms have been extensively studied and reviewed (Nisar et al., 2015; Concepcion et al., 2018; Zhai et al., 2016; Sun et al., 2018). The first committed step of carotenoid biosynthesis is the formation of phytoene from the condensation of two geranylgeranyl diphosphate molecules is the first committed step and is catalyzed by phytoene synthase (PSY). In higher plants, phytoene is converted to all-*trans* lycopene by phytoene desaturase (PDS), ζ-carotene isomerase (ZISO), ζ-carotene desaturase (ZDS) and carotene isomerase (CRTSIO) (Park et al., 2002; Bartley et al., 1991; Chen et al., 2010; Dong et al., 2007). However, in bacteria, the desaturation and isomerization of phytoene to all-

trans lycopene is catalyzed by a single enzyme, CrtI (Fraser et al., 1992). Lycopene is then cyclized to form either β-carotene (β-ring, β-ring) or α-carotene (ε-ring, β-ring) (Harjes et al., 2008). Lutein is produced from α-carotene by the addition of hydroxyl groups catalyzed by ring-specific hydroxylases and β-carotene is converted to zeaxanthin via the mono-hydroxylated intermediate β-cryptoxanthin (Vallabhaneni et al., 2009). The β,β xanthophylls can be further modified via epoxidation and introduction of an allenic bond (a carbon atom having double bonds with each of its two adjacent carbon atoms) to form antheraxnathin, violaxanthin and neoxanthin. The formation of these products is generally viewed as the end point of carotenogenesis, but in nonphotosynthetic tissues, lutein and other xanthophylls can occur in their free form, or as mono- or diesters, with a fatty acid esterified to one or both ends of the molecule, respectively. The mechanisms underlying xanthophyll esterification remain undefined, with thus far no enzyme identified for this process.

Xanthophyll esters occur in flower petals, senescent leaves and in many commonly consumed fruits and vegetables such as chili peppers, oranges, potatoes and sqaush (Mercadante et al., 2017). They are also present in animal tissues including human skin (Wingerath et al., 1998) and colostrum (Ríos et al., 2017), avian ornaments (García-de Blas et al., 2013) and the shells of marine crustaceans (Wade et al., 2005).

Esterification increases the stability of xanthophylls both in vitro during UV (Subagio et al., 1999) and heat treatments (Subagio et al., 1999; Fu et al., 2010; Subagio and Morita, 2003) and in vivo in a range of plant tissues, including cereal grains, fruits, tubers and flowers of a range of species. Esterified carotenoids from paprika were more stable than their nonesterified counterparts after thermal treatment and storage (Schweiggert et al., 2007) and against lipoxygenase-catalyzed co-oxidation (Biacs et al., 1989). Similarly, zeaxanthin esters were determined to be the most thermostable pigments after Pasteurization of tamarillo fruits with esterified β-cryptoxanthin showing a higher retention after pasteurization than its unesterified equivalent (Mertz et al., 2010).

In harvested cereal grains, esterified lutein persists longer than free lutein (Ahmad et al., 2013; Mattera et al., 2015; Mellado-Ortega et al., 2016). For example, the decay rate for lutein monolinoleate at 37°C was one-third the rate of its free lutein counterpart (Mellado-Ortega and Hornero-Méndez, 2017). By promoting the retention of xanthophylls, esterification may modulate oxidative stress in seeds and other tissues, suppressing reactive oxygen species (ROS). It is well

documented that the antioxidant status of seeds influences ripening, viability and germination (Bailly, 2004; Sattler et al., 2004). Further, carotenoid accumulation has been reported to be positively correlated with shelf-life of cassava roots (Beyene et al., 2018). The antioxidant benefits of xanthophyll retention may explain why xanthophyll esterification occurs in a wide variety of plant species, both wild and cultivated.

Esterification has been postulated to increase carotenoid stability by aiding the sequestration and integration of xanthophylls into specialized lipoproteins called fibrils or into specialized membranous structures within plastids called plastoglobules. Sequestration into these structures protects carotenoids from oxidizing environments, enzymes involved in carotenoid turnover and aids in preventing metabolic feedback. In vitro fibril reconstitution assays have demonstrated that fibril assembly is promoted by xanthophyll esters and inhibited by acyclic nonesterified carotenoids such as lycopene (Deruère et al., 1994). Association of xanthophyll esters with plastoglobules has been demonstrated using a tomato mutant that is unable to produce xanthophyll esters. This mutant displays reduced carotenoid accumulation as well as a reduced number of fully developed plastoglubules in petals (Ariizumi et al., 2014). This is further supported by a study investigating nonendogenous ketocarotenoids produced in transgenic tomato fruits which found that these esterified carotenoids preferentially associate with plastoglobules (Enfissi et al., 2019).

Lutein accumulates in the starchy endosperm, aleurone and embryo tissues of mature wheat grain (Ndolo and Beta, 2013) and is the only carotenoid that is detectable above trace levels (Howitt and Pogson, 2006; Howitt et al., 2009). Hexaploid bread wheat (*Triticum aestivum*) can contain lutein in both its free and esterified forms, with most accessions containing a substantial proportion of esterified lutein (Kaneko et al., 1995; Ahmad et al., 2013; Paznocht et al., 2018). Among 138 hexaploid wheat cultivars, only nine were found to contain exclusively free lutein (Kaneko and Oyanagi, 1995). These nine zero-ester genotypes are all related by pedigree, suggesting that esterification is a process under genetic control. The inhibition of ester formation in bread wheat grain at high temperatures (Kaneko et al., 1995; Ahmad et al., 2013) further supports the hypothesis that lutein esterification is enzymatically catalyzed.

Genetic mapping in a bread wheat population derived from a cross between a high-ester line (Sunco/Indis.82) and a zero-ester cultivar (Haruhikari) attributed the lutein esterification phenotype to a locus (*Lute*) on the short arm of chromosome 7D (Ahmad et al., 2015). This

genomic location is consistent with the lack of lutein esters both in nullisomic-tetrasomic genetic stocks that lack chromosome 7D (Ahmad et al., 2015) and in durum wheat (*T. turgidum* ssp. *durum* (Desf.)), which lacks the D genome. Mattera et al. (2015, 2017) independently demonstrated that the presence of chromosome 7D is necessary for lutein esterification by investigating a set of wheat genetic stocks which included disomic substitution lines. Similarly, the high yellow pigment in the grain of tritordeum (×*Tritordeum* Ascherson et Graebner), an amphidiploid of durum wheat and *Hordeum chilense* has been partially attributed to a locus for lutein esterification on chromosome $7H^{ch}$ (Mattera et al., 2015, 2017). The only other locus that has been reported to affect lutein esterification is a quantitative trait locus on bread wheat chromosome 2B (Sunco/Tasman population) (Howitt et al., 2009) that influences the extent of esterification. In tomato, mutations in the lysophospholipid acyltransferase (LPAT)-like domain of the *pale yellow petal 1* (*pyp1*) gene can prevent esterification of violaxanthin and neoxanthin in petals (Ariizumi et al., 2014).

Because carotenoid content is determined by the balance between the rates of synthesis and degradation, understanding the molecular mechanisms governing carotenoid esterification will likely aid the development of improved crop varieties with higher carotenoid contents. However, the genes and biochemical mechanisms underpinning xanthophyll esterification remain largely unknown, and were thus the focus of this investigation. Here, we report a gene, *Xat*, as the causative gene for esterification in the *Lute* locus on chromosome 7D of bread wheat. Using disomic substitution lines of durum wheat, we demonstrate that the presence of chromosome 7D is sufficient to enable lutein esterification in the grain of durum wheat. Using TILLING mutants in bread wheat, we demonstrate that *Xat* is essential for lutein esterification in the grain of bread wheat. Using in vitro assays with recombinant protein, we confirm the esterification activity of XAT and establish that the enzyme has a broad substrate specificity for both xanthophylls and acyl-donor substrates. We also demonstrate that XAT can esterify xanthophylls when expressed heterologously in rice embryogenic callus and present evidence that subcellular partitioning between XAT and its substrates may regulate the timing of lutein esterification. The results of this research extend knowledge of carotenoid biosynthesis beyond lutein to incorporate molecular components of xanthophyll esterification.

RESULTS

Chromosome 7D Confers the Ability to Esterify Lutein

To confirm the functionality of the 7D locus in lutein esterification, we investigated 7D(7A) and 7D(7B) disomic substitution lines of the durum wheat cultivar Langdon. Durum wheat, which is tetraploid and lacks the D genome, does not normally esterify lutein. In the Langdon 7D(7A) and 7D(7B) lines (Joppa and Williams, 1988), a pair of chromosomes (7A or 7B, respectively) have been replaced by 7D chromosomes from Chinese Spring hexaploid wheat, which does accumulate lutein esters in the grain. As expected for tetraploid wheat, Langdon was found to contain both all-*trans* and *cis*-isomers of free lutein, but no lutein esters (Table 1) and other carotenoids, including β-carotene and α-carotene, were present only at trace levels. In contrast, most (60-70%) of the lutein in the 7D(7A) and 7D(7B) substitution lines was present as lutein esters (Table 1). Consistent with published reports on lutein stability, the total *trans*-lutein content after 60 d at 37°C was significantly higher in the disomic substitution lines than in Langdon.

XAT is Essential for Lutein Esterification in Wheat Grain

The *Lute* locus on chromosome 7D was found to cosegregate with three genetic markers, *gwm295*, *wPt-3727* and *wPt-1163* (Ahmad et al., 2015). On the 7D pseudomolecule sequence, of the wheat genome assembly, these markers span a physical interval of 2.9 Mb (IWGSC RefSeq v1.0) (Figure 1A). One of the many open reading frames in this interval, TraesCS7D01G094000 (UniProt W516C5), shares homology with the GDSL esterase/lipase (GELP) gene family. The GELP family, which has over 110 members in rice (Chepyshko et al., 2012), encompasses multiple clades of enzymes with activities ranging from deacetylases (Zhang et al., 2017) to acyltransferases (Kikuta et al., 2012; Yeats et al., 2012). TraesCS7D01G094000 aligns most closely with clade IV (Chepyshko et al., 2012) (Figure 1B) for which ascribed activities include biosynthesis of cutin, which is produced via an acyltransferase reaction and is responsible for the waxy cuticle on the surface of aerial plant tissues (Yeats et al., 2012, 2014). Given that esterification is likely to be an acyltransferase reaction, this gene seemed worthy of further investigation.

TraesCS7D01G094000 is predicted to have a five-exon gene structure that encodes a 351 amino acid protein (Figure 1A). The zero-ester cultivar Haruhikari has a deletion beginning in the 4th intron of *Xat* and spanning into the intergenic region. When this presence/absence polymorphism was assayed using the Sunco/Indis.82//Haruhikari mapping population, products could only be

amplified for the high-ester lines and not for the zero-ester lines (Ahmad et al., 2015). Similarly, in a preliminary qualitative PCR analysis, transcripts were detected during caryopsis development in high-ester lines but not in zero-ester lines. Analysis of a publicly available RNA-seq data set (Ramírez-González et al., 2018) further revealed that TraesCS7D01G094000 is expressed in the developing caryopsis with high abundance in the endosperm with no detectable expression in vegetative tissues such as leaves or roots (Figure 2A). To investigate the spatial and temporal distribution of transcripts in grain, we undertook in situ mRNA hybridization on transverse sections of developing caryopses of the ester-accumulating cultivar Gladius (Figure 2B, i-iv). Early in caryopsis development (7 d after pollination; DAP), transcripts were particularly abundant in dividing endosperm nuclei, developing testa cells and differentiating aleurone layers (Figure 2B, i). Later in development, during the cell differentiation of endosperm (12-13 DAP and 21-22 DAP), transcripts remained enriched in cells of the aleurone layer and in starchy endosperm cells (Figure 2B, iii and iv). This is consistent with reports of lutein esters in endosperm tissue dissected from wheat grains (Ahmad et al., 2013). In contrast, signal levels detected in the zero-ester cultivar Haruhikari and the zero-ester double haploid line DM06.6*008 were similar to background levels observed in negative controls with no probe and no antibody (Figure 2, v-viii), indicating that the deletion in the Haruhikari allele leads to nonsense-mediated transcript decay.

To confirm whether TraesCS7D01G094000 is the causal gene for lutein esterification in the *Lute* locus, we screened a targeted induced local lesions in genomes (TILLING) mutant population derived from the bread wheat cultivar Gladius. This cultivar accumulated 59 ± 1 % esterified lutein out of the total carotenoid pool (n = 9). The remainder of the carotenoid pool was free lutein (as either all-*trans* or *cis*-isomers), with all other carotenoids, including β-carotene and α-carotene, either not detectable or at trace levels. Six independent mutations in TraesCS7D01G094000 (two truncation mutations, two missense mutations and a splice variant) resulted in the complete loss of lutein esters in grain harvested from plants homozygous for these mutations (Table 2). Two other mutations (both missense mutations) reduced lutein esters to 61-65% of that observed in the wild type Gladius cultivar (Table 2). For a missense mutation (G164A) that conferred complete loss of function in the homozygous state, all three possible genotypic classes (homozygous wild type, heterozygous and homozygous mutant) were obtained among self-pollinated M_3 progeny from a heterozygous M_2 plant (ga483). In this family, the level of lutein esters was high (97 ± 0.03% of Gladius, n = 2) for M_4 grains harvested from the homozygous wild type M_3 plants and intermediate

(65%, n = 2) for M_4 grains harvested from heterozygous plants. Similarly, the level of lutein esters was 55 ± 0.05% (n = 4) of Gladius for M_4 grains harvested from M_3 plants that were heterozygous for the splice mutation (G511A). Considering that the allelic dosage in the endosperm of M_4 grains harvested from heterozygous M_3 plants would range from 0 to 3, with an expected mean of 1.5, the intermediate phenotypes are consistent with expectations. We conclude that TraesCS7D01G094000 is genetically necessary for lutein acyltransferase activity and herein refer to the encoded protein as xanthophyll acyltransferase (XAT) and the gene as *Xat*.

XAT Catalyzes the Synthesis of Xanthophyll Esters

In order to verify enzymatic activity, recombinant XAT minus the putative 21-amino-acid signal peptide, was purified from *Escherichia coli* (Supplemental Figure 1). When assayed with lipids extracted from flour of a zero-ester wheat line (DM06.6*048), the purified XAT exhibited time-dependent esterification of a free-lutein standard (Figure 3A). The recombinant enzyme showed significant acyltransferase activity that varied by less than 2-fold across a broad temperature range, displaying maximum activity at 37°C (n = 3) (Figure 3B) and a broad pH range (Supplemental Table 1). Esterified compounds were separated from free lutein via HPLC and confirmed as lutein esters by an alkaline hydrolysis saponification reaction to form free lutein (Figure 3A, inset). Thus, recombinant XAT is sufficient to catalyze lutein esterification using lipids extracted from a XAT-deficient, zero-ester line.

Members of the GDSL esterase/lipase family contain a conserved Ser residue within the GDSL motif that is located near the N-terminus. This Ser serves as a nucleophile in a catalytic triad consisting of the Ser in the Block I domain and Asp and His residues in the Block V domain (Akoh et al., 2004). Alignment of XAT protein sequence homologs from multiple plant species revealed conservation of this triad (Figure 3A). In order to verify function of the conserved catalytic triad in XAT, site-directed mutagenesis was employed to substitute Ala for the conserved Ser-37 in Block I and the mutated recombinant protein was purified (Supplemental Figure 1). The resulting S37A substitution completely abolished lutein esterification activity, confirming that the Ser-37 residue is an integral part of the catalytic triad required for XAT function (Figure 3B).

Triacylglycerides Are the Preferred Substrate for XAT

Given the broad range of chemical reactions carried out by GDSL esterase/lipase enzymes (Akoh et al., 2004), defining the chemical reaction catalyzed by XAT requires identification of the substrate that is the acyl donor. Assays were performed in which purchased standards of major lipid classes (5 mM concentration) were incubated with 40 μM lutein and 20 μg of XAT. All lipid standards contained either linoleic and/or palmitic acids, the main fatty acids esterified to lutein in wheat grain (Ahmad et al., 2013; Mellado-Ortega and Hornero-Méndez, 2015; Kaneko et al., 1995). While XAT was able to accept all of the lipid substrates tested except phosphatidylcholine, triacylglycerides (TAGs) were determined to be the preferred substrate (Table 3), indicating that XAT functions via a transesterification mechanism (Figure 4B). To explore the xanthophyll acyl acceptor specificity of XAT, two additional nutritionally relevant xanthophylls (zeaxanthin and β-cryptoxanthin) were tested. With pure trilinolein as the acyl donor, XAT esterified all substrates tested: zeaxanthin and β-cryptoxanthin and free lutein as a control (Figure 4A).

We performed further kinetic analysis of XAT incubated for 4 h with lutein and the favored acyl donor, trilinolein, after verifying that our reaction conditions permit measurement of the initial velocity of the enzyme at this set time point (Supplemental Figure 2A). The data were fitted to a nonlinear regression analysis to calculate K_m and V_{max} (Supplemental Figures 2B and 2C). The K_{ms} for lutein and trilinolein were determined to be 60.3 ± 7.6 and 50.6 ± 27 μM, respectively. These values are comparable to those of a previously reported GDSL esterase/lipase that has acyltransferase activity (Kikuta et al., 2012) (Table 4). The K_m values determined for the two substrates are not significantly different, indicating that XAT binds to both substrates with similar affinity.

XAT Is Localized to the Apoplast During Caryopsis Development

The rice homolog of XAT, Os06g148200, was previously detected in the secreted fraction of proteins from callus suspension culture cells (Cho et al., 2009). In agreement with this observation, analysis of the XAT signal peptide using SignalP 4.0 software (Petersen et al., 2011) predicted XAT to be localized to the apoplast. This was surprising, given that carotenoid biosynthesis occurs exclusively within the plastids of plant species. To assess the localization of XAT in planta, a series of mCherry fusion proteins were constructed, varying the location of the mCherry in order to

mitigate against the limitations in interpretation of a single fusion (Millar et al., 2009). Constructs were transiently transformed into *Nicotiana benthamiana* leaves, and colocalized with markers for known subcellular locations. Given the presence of a predicted signal peptide on the N-terminus of XAT, a fusion construct was made with mCherry inserted between the predicted signal peptide and the remainder of the *Xat* coding sequence (SP-mCherry-XAT) to avoid masking the targeting signal. In *N. benthamiana* leaves, SP-mCherry-XAT failed to substantially colocalize with known markers for the endoplasmic reticulum or the plasma membrane (Figure 6, Supplemental Figures 3 and 4) and was mostly restricted to a region outside of these markers, implying that it is localized to the apoplastic region. Plots of the fluorescence from mCherry and plasma membrane marker (Figure 6, Supplemental Figures 3 and 4) further support this conclusion. In some cases, a low level of intracellular signal was detected compared to the apoplastic signal, which we interpret as newly synthesized fusion protein undergoing synthesis and secretion. A control, consisting of only the predicted signal peptide of XAT, fused to mCherry, resulted in similar localization compared to the internal SP-mCherry-XAT, further corroborating that this construct is localized to the apoplast (Figure 6, Supplemental Figure 4). As a second control, a C-terminal fusion, XATΔSP-mCherry with the N-terminal signal peptide removed, was also constructed. The mCherry signal from this construct was retained in the cytoplasm and the nucleus, indicating that the N-terminal predicted signal peptide is essential for correct localization of XAT (Supplemental Figure S3). Interestingly, a C-terminal fusion with the signal peptide, SP-XAT-mCherry, was highly colocalized with an endoplasmic reticulum marker, implying that C-terminal modifications or interactions are required for apoplastic localization of XAT (Supplemental Figure S3).

XAT has Esterase and Lipase Activity

The localization of XAT to the apoplastic region raises the question: does XAT have any other enzymatic function in addition to catalyzing the esterification of xanthophylls? As *Xat* is a member of the GDSL esterase/lipase gene family, we assayed it for esterase and lipase activity with *p*-nitrophenyl esters as substrates. These synthetic substrates have previously been used to test the esterase and lipase activity of other characterized GDSL esterase/lipases (Zhang et al., 2017; Kikuta et al., 2012; Lee et al., 1997; Oh et al., 2005). Recombinant XAT was able to catalyze the hydrolysis of both the short-chain (*p*-nitrophenyl acetate, p-NPA) and long-chain (*p*-nitrophenyl palmitate, p-NPP) substrates, demonstrating that XAT has both esterase and lipase activity,

respectively. XAT was further determined to have saturable kinetics with these substrates (Supplemental Figures 5A and B) yielding K_m values of 474 ± 94 and 160 ± 67 μM for p-NPA and p-NPP, respectively (Table 3.3). These values are approximately 3-fold (pNPP) and 8-fold (pNPA) higher than the K_m constants determined for lutein and the TAG substrate, trilinolein, when XAT follows a transesterification mechanism. This indicates that lutein and TAGs are competitively binding and are preferred substrates of XAT. To further explore the preference of XAT for the substrates of transesterification activity over hydrolysis, the reaction rate of XAT-mediated hydrolysis of pNPP was investigated with the addition of lutein as a competitive substrate. If XAT has similar affinities for lutein and pNPP, we would expect that the addition of an equimolar concentration of lutein would reduce the rate of pNPP hydrolysis to approximately 50% of the control reaction. However, the addition of 2 mM lutein reduced the rate of pNPP hydrolysis to 33 ± 2% of the control reaction with 2mM pNPP (Supplemental Figure 5C), again indicating lutein as a preferred substrate of XAT.

Given that XAT is able to function as a lipase, it was important to determine if XAT can hydrolyze xanthophyll esters in addition to synthesizing them. Esterified xanthophylls were extracted from marigold petals (*Tagetes patula* cv. Red) and purified via HPLC. Marigold petals were chosen because they are a good source of lutein esters that have a high quantity of lutein esterified to palmitic acid (16:0) as well as a significant proportion of lutein esterified to myristic (14:0) and stearic acids (18:0) (Abdel-Aal and Rabalski, 2015; Li et al., 2007). After a 4-h incubation of the marigold xanthophyll ester extract with recombinant XAT, no release of free xanthophylls could be detected (Figure 7). In contrast, a control enzyme, lipase type VII from *Candida rugosa* (EC 3.1.1.3), previously shown to hydrolyze xanthophyll esters (Breithaupt et al., 2002) was able to hydrolyze a proportion of xanthophyll esters releasing free lutein and a smaller proportion of other free xanthophylls under the same reaction conditions (Figure 7). Therefore, whereas XAT can act as an esterase and lipase as shown via assays with *p*-nitrophenyl esters (Supplemental Figure 5), it is unlikely to hydrolyze the products of its acyltransferase activity, the xanthophyll esters. However, whether XAT is involved in a hydrolysis reaction either in as an esterase or a lipase and the identity of any other endogenous substrates in developing wheat grain remain to be determined.

The *Xat* Transgene Induces Synthesis of Xanthophyll Esters in Rice Callus

As the aforementioned activity assays were all in vitro, we sought to determine if XAT is sufficient to induce production of xanthophyll esters in vivo when coexpressed and colocated with xanthophylls. Rice embryogenic callus has previously been used as a model system for functional characterization of carotenoid metabolism genes (Bai et al., 2014). A series of constructs were generated to recreate carotenoid biosynthesis in combination with XAT in rice embryogenic callus (Figure 8A). The constructs included the hygromycin phosphotransferase gene (HPT) to confer hygromycin resistance, maize phytoene synthase 1 (ZmPSY1), bacterial phytoene desaturase (CrtI), *β-CAROTENE HYDROXYLASE* 2 from *Arabidopsis thaliana* (AtBCH2) and wheat *Xat* in which the signal peptide was substituted for the transit peptide from the Arabidopsis ribulose-1,5-bisphosphate carboxylase/oxygenase small subunit (SSU) to target the enzyme to the plastid. All genes were constitutively expressed: the *HPT* selectable marker and *CrtI* were controlled by the rice actin promotor; *ZmPSY1* and *AtBCH2* by the *Panicum* ubiquitin promotor; and SSU-*Xat* by the maize ubiquitin promotor. Constructs were transformed into rice embryogenic callus using *Agrobacterium tumefaciens* following the protocol described by Hiei and Komari (2006). Transformed rice calli exhibited a range of phenotypes from yellow to deep orange observable in all three genotypes, whereas untransformed callus was an off-white color (Figure 8A). For each construct, over ten independent lines were generated. HPLC analysis of transformed callus revealed that *AtBCH2* lines without XAT produced nonesterified xanthophylls, but mainly β-carotene, while no detectable carotenoids were observed in the untransformed callus (Figure 8B**)**. Only the line containing the plastid-targeted XAT was able to produce xanthophyll esters (Figure 8B, inset). Additional peaks observed in the SSU-XAT expressing line were further confirmed as xanthophyll esters via saponification treatment which returned the xanthophylls to their free forms (Figure 8C). Saponification treatment also revealed that in addition to lutein and β-cryptoxanthin, other xanthophylls which were not assayed in vitro as acyl-acceptor substrates of XAT were also esterified including neoxanthin and violaxanthin. We quantified the total carotenoid content of the transgenic rice callus lines in order to determine if expression of *Xat* influenced carotenoid metabolism and flux into the pathway (Supplemental Figure 6). No difference in total carotenoid content could be detected between lines overexpressing *Xat* and those without the transgene.

DISCUSSION

The occurrence of xanthophyll esters is widespread throughout nature, especially in flowers and commonly consumed fruits (Mercadante et al., 2017). Lutein is also regularly found esterified in the grain of wheat species including bread wheat, spelt (*Triticum spelta*), einkorn (*Triticum monococcum*) and tritordeum (x *Tritordeum* Aschers. et Graeb.) (Ziegler et al., 2015). Due to the high consumption of fruits and cereals, a significant proportion of carotenoids are ingested in their esterified forms. However, despite their widespread occurrence and dietary impact, the molecular mechanisms underpinning xanthophyll esterification have remained elusive in all plant species. The esterification of lutein in bread wheat has been proposed to be an enzymatic process for over two decades (Kaneko et al., 1995). Here, we have identified that a xanthophyll acyltransferase encoded by a gene on the short arm of chromosome 7D is essential for the esterification of lutein in the endosperm of bread wheat and further provide detailed analysis of biochemical parameters of the function of this enzyme.

Genetic Evidence of XAT Function

Durum disomic substitution lines that carry the 7D chromosome of bread wheat were found to express the lutein-ester phenotype that is absent from wild-type durum (Table 1). This provided gain-of function evidence at the chromosome level. To obtain evidence at the gene level, we screened a TILLING population for mutations in the candidate gene on the short arm of chromosome 7D. We discovered six independent mutations in *Xat*, all of which conferred the zero-ester phenotype, and two missense mutations with partial activity (Table 2). We can therefore conclude that XAT is the only functional xanthophyll esterifying enzyme in bread wheat. Given the hexaploid nature of the bread wheat genome, it is interesting that there appear to be no functional homoeologues. The high yellow pigment content in the grain of *Tritordeum*, a hybrid of durum wheat and *H. chilense*, is in part due to a locus for lutein esterification found on the $7H^{ch}$ chromosome (Mattera et al., 2017, 2015). The causative enzyme encoded in this locus is thought to be complementary to the enzyme encoded on the 7D chromosome of bread wheat, now determined to be XAT, as they show different preferences for acylation on the β- and ε- rings of lutein (Mattera et al., 2017). However, the regiospecificity of XAT was not investigated in the present study. With respect to the 2B locus of bread wheat identified in an earlier study (Howitt et

al., 2009) we conclude this is not enzymatic due to the complete lack of esters in TILLING lines lacking *Xat* that still contain the 2B locus; more likely it indirectly affects the amount of ester accumulation. Heterologous expression of *Xat* in rice embryogenic callus further provides gain-of-function evidence, with xanthophyll esters produced only in lines expressing a plastid-targeted *XAT* (Figure 8B).

XAT Transesterification Requires Ser-37 in the GDSL motif

Proteins containing a GDSL motif are ubiquitous in the plant kingdom and are present in large gene families (Volokita et al., 2011). The GELP family, which has 114 members in rice and 108 members in Arabidopsis, encompasses multiple clades of enzymes with functions ranging from esterase (Huang et al., 2015) and lipase activity (Hong et al., 2008) to deacetylase (Zhang et al., 2017) and acyltransferase (Kikuta et al., 2012; Yeats et al., 2012) activity. Phylogenetic analysis revealed that XAT aligned to clade IV of the previously generated rice GDSL esterase/lipase family phylogenetic tree (Chepyshko et al., 2012). This clade also includes the rice homolog of the CD1 enzyme which functions via transesterification (Yeats et al., 2014, 2012) (Figure 1B). On the other hand, the previously characterized rice BS1 enzyme, which has hydrolytic activity (Zhang et al., 2017), groups with clade I of the GDSL esterase/lipase phylogenetic tree. Within clade IV, XAT clusters with its own homologs and not with other GDSL esterase/lipases (Figure 1B) which indicates that other GELP family members in rice are unlikely to share substrates with XAT and are hence unlikely to act upon xanthophylls.

A distinguishing feature of members of the GDSL family is that their Ser-containing motif is located close to the N-terminus. This is in contrast to classical lipases, in which the GxSxG motif is near the center of the protein sequence (Akoh et al., 2004). As expected for GDSL enzymes, mutating the conserved serine (Ser-37) present in the GDSL motif of XAT completely abolished esterification activity (Figure 3B), confirming the role of Ser-37 in the catalytic triad of the active site. Further, no lutein esters were detected for two TILLING mutant lines with premature stop codons (ga1112 with Q131stop; ga236 with Q194stop; Table 2). These lines would be expected to provide truncated forms of XAT that lack the C-terminal Asp-326 and His-329 residues that are required for catalysis. Two independent missense TILLING lines (ga243 and ga483, Table 2), both with a D40N substitution, exhibited the zero-ester phenotype. Given the location of this residue

near the GDSL motif and the active-site Ser, this mutation may alter the shape of the active site pocket and therefore the binding of substrates. Further experimentation is needed to confirm this.

Considering that GDSL-motif enzymes have a flexible substrate binding pocket (Akoh et al., 2004), it is not surprising that XAT can employ multiple acyl-donor and acyl-acceptor substrates. XAT was found to have broad acyl-donor and xanthophyll substrate specificity, esterifying not only lutein, but two other nutritionally important xanthophylls; zeaxanthin and β-cryptoxanthin (Figure 4A). The preference for TAGs as the acyl donor for XAT (Table 3) is consistent with the enzyme esterifying xanthophylls via a transesterification mechanism (Figure 4B). Whereas most GDSL-motif enzymes have esterase (Oh et al., 2005; Clauss et al., 2008) or lipase activity (Kim et al., 2008; Hong et al., 2008), several characterized family members have acyltransferase (Kikuta et al., 2012) or transesterification activity (Yeats et al., 2012, 2014). TAGs are the most abundant class of lipid in the nonstarch fraction of wheat endosperm, accounting for approximately 46% of the total nonstarch lipid content (Morrison, 1978). The main fatty acid constituents of TAGs in the endosperm of bread wheat are linoleic acid (18:2), palmitic acid (16:0) and oleic acid (18:1) which account for 57-65%, 13-20% and 13-17% of the TAG fatty acid composition, respectively (Morrison, 1978). Therefore, the fatty acid profile of TAGs, the preferred acyl donor for XAT, correlates to the fatty acids esterified to lutein in mature wheat grain. This is in contrast to the fatty acids esterified to xanthophylls in potatoes (Breithaupt and Bamedi, 2002; Fernandez-Orozco et al., 2013) and capsicum fruits (Minguez-Mosquera and Hornero-Mendez, 1994) which do not correlate to the fatty acid profile of the total lipid pool. This would suggest that the yet unidentified enzyme/(s) catalyzing xanthophyll esterification in these species may be more discriminatory in the type of acyl donor.

In tomato, a study of the *pyp1* (pale yellow petal 1) mutant led to the identification of the PYP1 gene as essential for the esterification of violaxanthin and neoxanthin in petals with saturated fatty acids (Ariizumi et al., 2014). Mutations in the acyltransferase domain of PYP1 resulted in loss of xanthophyll esters and a disruption in carotenoid sequestration, leading to a reduced total carotenoid pool and altered chromoplast development. However, no catalytic activity was demonstrated. PYP1 contains a lysophospholipid acyltransferase (LPAT)-like domain, whereas XAT contains a GDSL esterase/lipase motif. In silico analysis of *PYP1* failed to predict localization of the encoded protein to the plastid, but this has not been validated experimentally.

Recently, a PYP1 homolog, denoted ripening-specific acyl-transferase (rsAcT) from chili pepper (*Capsicum annuum*) was identified (Berry et al., 2019). The authors reported the onset of xanthophyll esterification in chili pepper fruit coincided with the expression of *rsAcT* and the cessation of ripening similarly corresponded with a decrease in transcript abundance. Although there is genetic evidence that PYP1 is required for xanthophyll esterification in tomato petals and correlative evidence that rsAcT might be involved in esterification in *Capsicum* fruit, experiments providing evidence of activity and subcellular localization of these enzymes have yet to be conducted. Hence, it remains to be seen if PYP1 and rsAcT are sufficient for esterification and can indeed catalyze the formation of xanthophyll esters.

Localization of XAT to the Apoplastic Region: a Method of Subcellular Partitioning

It is well established that although carotenoid biosynthetic genes are encoded in the nuclear genome, the mature proteins are localized to and function within plastids (Shumskaya and Wurtzel, 2013)**.** It was therefore curious to find that XAT is localized to the apoplastic region (Figure 6) rather than the site of carotenoid accumulation. XAT is the first GELP family enzyme to be associated with carotenoid metabolism and the first reported carotenoid metabolism enzyme found to be localized outside of plastids. One member of the carotenoid cleavage dioxygenase family, CCD1, is localized to the cytoplasm (Auldridge et al., 2006). However, it is presumed to function on mobile apocarotenoids, not on carotenoids per se. In higher plants, carotenoids are not detected outside intact plastids. However, the alga *Haematococcus pluvialis* synthesizes photosynthetic carotenoids within the chloroplast during the active phase of its life cycle. Then, in response to stress, it accumulates astaxanthin esters in the cytoplasm of dormant cysts (Boussiba, 2000). Experiments with extracted subcellular compartments from *H. pluvialis* fractionated via a sucrose gradient indicated that the esterification of astaxanthin occurs within the endoplasmic reticulum (Chen et al., 2015).

Our mRNA expression and enzyme localization evidence presents two paradoxes. Firstly, *Xat* mRNA appears during grain development yet lutein ester formation does not occur until after grain desiccation. Secondly, during grain development, lutein is localized in the amyloplast but XAT is localized in the apoplastic region. The former could simply reflect an uncoupling of mRNA and protein accumulation, but when considered with the second observation, a hypothesis emerges that the subcellular partitioning of enzyme and substrates provides a distinctive mechanism that

regulates the timing of lutein esterification in wheat grain. As wheat grain matures, the starchy endosperm cells undergo programmed cell death, resulting in degradation of nuclear DNA and loss of membrane integrity (Domínguez and Cejudo, 2014). This could allow XAT access to lutein, which is otherwise localized to different subcellular compartments during caryopsis development. Lutein ester production in cereal grain increases in response to heat with a maximum rate at approximately 80°C (Ahmad et al., 2013; Mellado-Ortega et al., 2015). In vitro, recombinant XAT enzyme had activity across the wide range of temperatures examined and the optimal temperature was 37°C (Figure 2B). Thus, the observation of increased lutein esterification in mature wheat grain at elevated temperatures is consistent with the hypothesis that increasing temperature exacerbates cellular damage in stored wheat grain, further facilitating XAT access to substrates. High temperatures may also facilitate release of lipids present in spherosomes (oil droplets) allowing for higher availability of acyl donors, in turn increasing the rate of the transesterification reaction. It should also be noted that XAT retained around 50% activity at the highest temperature investigated, 64°C (Figure 2B), and activity varied by less than 2-fold over a broad pH range (5.0-10.0) (Supplemental Table 1). This indicates that XAT is highly stable and would therefore be able to function within the highly oxidative environment of desiccating grain.

Regulation of protein activity by subcellular partitioning is not without precedent. For example, nuclear-cytoplasmic partitioning is known to contribute to regulation of levels of the stem-cell-promoting transcription factor WUSHEL in the inflorescence meristem of *Arabidopsis thaliana* (Rodriguez et al., 2016). Specialized secondary metabolism is often spatially partitioned between cell types, as is the case for the production of unique alkaloids in species such as *Catharanthus roseus* for which catharanthine and vindoline are spatially separated with herbivory-induced cell damage promoting the formation of dimeric toxins (Roepke et al., 2010).

Esterification is a Key Function of XAT

Considering the subcellular separation of XAT from its substrates during grain development, it is intriguing to contemplate the physiological relevance of esterification being regulated by compartmentalization. Are there selective pressures that could have driven the evolution and retention of such an elaborate enzymatic mechanism, or is it more serendipitous? Indeed, the localization of XAT to the apoplast raises the question as to whether xanthophyll esterification is

a primary activity of the enzyme. In order to address this, kinetic analysis of the enzyme was performed with the substrates of transesterification (Table 4). XAT was determined to have K_m values within the submillimolar range for both lutein and TAG, and these values did not significantly differ from each other ($p>0.05$). The K_m values determined (60.2 ± 7.6 and 50.6 ± 27 μM for lutein and TAG, respectively) are either similar to or more favorable than calculated K_m values of previously characterized GDSL esterase/lipases. The enzyme TcGLIP1 from Dalmation pyrethrum (*Tanacetum cinerariifolium*) was determined to have similar K_m values ranging from 30 to 1050 μM depending on the substrates used during the in vitro production of pyrethrins (Kikuta et al., 2012). However, the CD1 enzyme, which produces cutin via transesterification of a specific monoglyceride, yielded an apparent K_m of 925 μM. Similarly, the BS1 enzyme from rice, which has hydrolytic activity, was found to have a K_m for its natural substrate of 4.4 mM and K_m values greater than 2.0 mM for synthetic substrates. The K_m values of XAT calculated for both lutein and TAG taken together with results from analysis of the TILLING population (Table 2) suggest that xanthophyll esterification is a key function of the enzyme.

To further explore possible functions for XAT, the esterase and lipase activity of the XAT were investigated because XAT is a member of the GDSL esterase/lipase family, of which many members are known to have hydrolytic activity (Hong et al., 2008; Oh et al., 2005; Huang et al., 2015). In addition to having acyl-transferase activity producing xanthophyll esters, XAT was able to hydrolyze ester bonds on both short and long chain synthetic *p*-nitrophenyl ester substrates (Table 4, Supplemental Figure 5). XAT is not the first multifunctional GDSL esterase/lipase enzyme characterized. The GDSL enzyme TcGLIP from *T. cinerariifolium,* which functions via transesterification during the production of pyrethrins, was also shown to have hydrolytic activity against short-chain nitrophenyl esters as well as the pyrethrin substrates it produces; albeit with a much lower affinity for the substrates of hydrolysis (Kikuta et al., 2012). The enzyme TAP from *E.coli* was also shown to be a multifunctional GDSL esterase/lipase acting as a thioesterase, protease, arylesterase, lysophospholipase and as an esterase (Lee et al., 2006; Huang et al., 2001). To determine whether the hydrolytic activity or the transesterification activity of XAT is its primary function, in vitro enzyme kinetic analysis was also performed on the synthetic substrates for hydrolysis (Supplemental Figure 5). The K_m of XAT for the nitrophenyl acetate and nitrophenyl palmitate substrates were found to be approximately 8- and 3- fold higher, respectively, than those calculated for lutein and the triglyceride substrates of the transesterification reaction (Table 4).

This indicates that XAT has a higher affinity for the substrates of its transesterification reaction again and is consistent with the esterification of lutein being a key role of this enzyme. Whilst XAT was shown to have esterase and lipase activity in vitro with synthetic substrates, it is still unknown whether the enzyme also has this function in vivo and what substrates, if any, it hydrolyses. One hypothesis is that the hydrolytic activity of XAT may facilitate the breakdown of cellular compartments to afford XAT access to lutein during grain maturation. This hydrolytic role however, is not likely to be essential for the production of wheat and wheat-based products. Whilst the majority of bread wheat accessions have some proportion of lutein in its esterified form (Kaneko and Oyanagi, 1995; Ahmad et al., 2015), the Japanese bread wheat variety Haruhikari, which lacks *Xat*, is a successful cultivar with high yield and good end-use quality (Kaneko et al., 1995; Tanaka et al., 2005). Similarly, no deleterious traits were observed in bread wheat lines lacking *Xat*, nor in durum wheat, which lacks the D genome entirely and hence lacks *Xat* and is a well-adapted and widely grown crop. Most GELP family enzymes that have been functionally analyzed in plants have roles relating to pathogen responses (Lee et al., 2009; Kikuta et al., 2012; Hong et al., 2008), cutin metabolism (Yeats et al., 2012, 2014; Takahashi et al., 2010; Li et al., 2017) or pollination (Updegraff et al., 2009), all of which are consistent with apoplastic localization and have pronounced phenotypes. This would indicate that if there is any other function for XAT within the apoplast, it is either not a core cellular process or is subject to functional redundancy or tissue-specific regulation in wheat. In this respect, it is of interest that *Xat* mRNA expression is largely restricted to developing grain and was not detected in vegetative tissues for wheat (Ramírez-González et al., 2018) (Figure 2A).

Given that XAT can cleave ester bonds as demonstrated with synthetic ester substrates, an assay was designed to investigate if XAT could also hydrolyze xanthophyll esters, performing the reverse reaction of its acyl-transferase activity. XAT, however, was unable to hydrolyze xanthophyll esters purified from marigold flowers (Figure 7). Given that xanthophyll esters are much larger molecules than the *p*-nitrophenyl esters, this most likely reflects steric hindrance obstructing the xanthophyll esters from reentering the enzyme active site.

To further assess the function of XAT we heterologously expressed plastid-targeted *Xat* in carotenoid-accumulating rice embryogenic callus to determine if esters will form in vivo when the enzyme is co-located and co-expressed with its substrate. Rice calli expressing SSU-XAT

were shown to accumulate xanthophyll esters (Figure 8B), indicating that XAT is able to function within plastids of undamaged cells. Saponification of the transformed calli (Figure 8C) further confirmed results of in vitro assays in which xanthophylls such as β-cryptoxanthin and zeaxanthin, that either do not accumulate or are produced in trace quantities in wheat, can be esterified via XAT activity (Figure 4A). Additionally, we quantified the total carotenoids produced in the transgenic rice callus lines to investigate whether introduction of *Xat* influences carotenoid metabolism (Supplemental Figure 6). No difference in carotenoid accumulation was observed between lines expressing *Xat* and lines without the transgene. Given the low levels of xanthophyll accumulation in the transgenic rice calli, any systematic evaluation of increased stability and sequestration of esterified carotenoids in rice would require substantial optimization of the expression systems. Saponification treatment also revealed that violaxanthin and neoxanthin, which were not assayed with XAT in vitro, can also be modified by this enzyme in rice calli. Significantly, heterologous expression in rice callus also demonstrated that XAT can produce xanthophyll esters in a species that normally contains exclusively free-xanthophylls.

Conclusion

Carotenoid accumulation in plant tissue is a complex process governed by the balance between the rates of synthesis and degradation. Given that esterification enhances the stability of xanthophylls (Subagio et al., 1999; Fu et al., 2010; Subagio and Morita, 2003; Schweiggert et al., 2007) and promotes their sequestration and accumulation (Ariizumi et al., 2014; Fernandez-Orozco et al., 2013), greater understanding of the mechanisms governing xanthophyll esterification should lead to new strategies for increasing the carotenoid content of crops targeted for biofortification. Whilst our genetic and biochemical evidence demonstrate that XAT is both necessary and sufficient for esterifying at least three nutritionally-relevant xanthophylls (lutein, zeaxanthin and β-cryptoxanthin), we cannot rule out the possibility that XAT has additional enzymatic functions in wheat grain. It is of interest that the substrates and enzyme are spatially separated within a cell leading to the proposition that apoplastic XAT is brought into contact with its carotenoid substrates as the wheat grain matures and the subcellular structures in endosperm cells deteriorate during programmed cell death. In conclusion, we classify XAT as the first member of the widely-distributed GDSL esterase/lipase family to be shown to be capable of catalyzing the formation of xanthophyll esters.

METHODS

Plant Material and Growth Conditions

Plant material used in this research for phenotypic and genotypic analyses were durum and hexaploid wheat cultivars and experimental lines, including the hexaploid wheat parents Haruhikari, Sunco/Indis.82 and two doubled haploid progeny lines (DM06.6*008 and DM06.6*048, neither of which produce lutein esters) derived from the F_1 generation of a cross between those parents (Ahmad et al., 2015), the durum wheat cultivar Langdon and its 7D(7A) and 7D(7B) disomic substitution lines with chromosome 7D from Chinese Spring (Joppa and Williams, 1988), and the hexaploid wheat cultivar Gladius and the M_3/M_4 TILLING mutants for *Xat*. Plants were grown in a controlled environment room for five months under a 22/16ºC 14/10 h light/dark photoperiod. Each plant was grown in a 15-cm pot filled with coco-peat and supplied with slow-release fertilizer granules (Scotts Osmocote, Australia). Spikes were bagged to prevent accidental cross pollination.

For phenotypic analysis of Langdon and its 7D(7A) and 7D(7B) substitution lines, mature grain was harvested from three individual plants per line for evaluation of lutein ester content.

Development and Screening of the Gladius TILLING Population

A mutagenized population of the bread wheat cultivar Gladius was developed and screened according to procedures as previously described (Dong et al., 2009; Sharp and Dong, 2014). A *Xat*-specific product was amplified using the primers XAT-L1, 5'-CTAGAGCAGTATCTTCTTGTCTTCTGG-3', and XAT-R1, 5'-CGAGAACCACAATCTTGAGATCATGG-3', then digested with CEL 1 endonuclease prepared from celery as described by Sharp and Dong (2014). Mutants were detected using agarose gel electrophoresis. PCR products of the mutants were purified and sequenced. For each line for which a missense, nonsense or splice mutation was detected, five M_3 seeds were sown. Each seedling was genotyped for the expected mutation using CEL 1 digestion. At maturity, grain was harvested from each plant for evaluation of lutein ester content.

Evaluation of Lutein Ester Content in Grain

Prior to analysis of lutein esters, grain samples were stored at 37°C in an airtight container over silica gel for at least 60 d. Carotenoids were extracted from wheat grain and analyzed on a C30 reversed-phase column (Ultracarb 5 μm C30, 250 × 4.6 mm; Phenomenex, Pennant Hills, NSW, Aust.) using HPLC (Hewlett Packard 1100; Agilent Technologies, Santa Clara, Calif., USA) equipped with a photodiode array detector as previously described (Ahmad et al., 2015). Samples were separated at 1 mL min^{-1} with a mobile phases of 81:15:4 methanol/MTBE/water (solvent A) and 90:10 MTBE/ methanol (solvent B). A gradient elution was performed with 100% solvent A for 10 min followed by a gradient to 50% solvent A by 40 min, then to 100% solvent B by 50 min and finally isocratic elution with 100% solvent B for 10 min. The column was prepared for the following run, as previously described (Ahmad et al., 2015). Lutein ester concentrations were calculated as free lutein equivalents and expressed as a percentage of total lutein. Analyses of variance for each data set were performed with significant differences indicated within each figure and table.

Preliminary Quantitative Real-time PCR

Total RNA of developing grains was extracted using TRIzol Reagent (Life Technologies, USA). RNA samples were treated with DNase I (QIAGEN) on-column at room temperature using cartridges supplied with PureLink RNA Mini Kit (Life Technologies, USA). RNA quality was checked on 1.0% agarose gel and was quantified with a NanoDrop spectrophotometer (ThermoFisher Scientific, USA). cDNA synthesis was performed using iScript cDNA synthesis Kit (Bio-Rad, USA) with oligo(dT) primer and random hexamers, TaqMan primers and a probe designed from a part of exon 3 that is present in both the Haruhikari and Sunco/Indis.82 alleles of *Xat*. The 27-nt probe sequence (ACAACTATTACATCAACCCTTTCCTCG) was 5'-labelled with 6-FAM and 3'-tagged with BHQ-1. The sense and antisense primer sequences were luteTaqMan_S (5'- GGTTCATGTGACTTTGTC-3') and luteTaqMan_AS (5'-CACTGTTGTTGAACATCC-3'), respectively. TaqMan assays were run on a LightCycler®480 (Roche) with KAPA Probe Master Mix (GeneWorks) used for the assays. Relative quantification using $2^{\wedge-\Delta\Delta CT}$ was used in normalization of gene expression against the Puroindoline b (*Pin b*) reference gene. Each qPCR reaction was run in triplicate.

mRNA in situ Hybridization

Probes were amplified from cDNA prepared from developing grains (6 DAP-36 DAP) of Chinese Spring bread wheat using PrimeSTAR® GXL DNA polymerase (TaKaRa). Primers for sense fragment were S1F_EcoRI, 5'-AGGGAGACCGGAATTCCCGGTTCATGTGACTTTGTCTACAACT-3' and S1R_HindIII, 5'-TATAGAATACAAGCTTAGGTAGCGAGGTTGTACAAAGGTGTA-3'. Primers for the antisense fragment were AS1F_EcoRI, 5'-AGGGAGACCGGAATTCAGGTAGCGAGGTTGTACAAAGGTGTA-3' and AS1R_HindIII, 5'-TATAGAATACAAGCTTCCGGTTCATGTGACTTTGTCTACAACT-3'. Amplicons were cloned into the pSPT18 vector using In-Fusion HD Cloning Kit (ClonTech). Transformants were selected on LB medium (0.1% [w/v] tryptone, 0.5% [w/v] yeast extract, 0.5% [w/v] NaCl, pH 7.0) supplemented with ampicillin (50 µg/mL). Inserts were verified by Sanger sequencing (Sanger et al., 1977). Probes were synthesized with DIG-labelled dUTP (T7/Sp6 RNA labelling kit, Roche, 1175025). Synthesized sense and antisense probes were assessed in a DIG-incorporation assay prior to mRNA in situ hybridization. The in situ hybridization protocol was modified from previous studies (Møller et al., 2009) as follows. Grain was harvested and fixed in FAA (50% [v/v] ethanol, 10% [v/v] paraformaldehyde [16% at EM grade], 5% [v/v] glacial acetic acid). Following dehydration, grain sections were infiltrated and embedded in paraffin wax. Embedded grain material was transversely cut into 7-µm sections and specimens were captured onto a poly-L-lysine-coated slide (Lomb SCIENTIFIC) using an RNase-free Leica rotary microtome. Paraffin wax was removed from tissue sections with HistoChoice (Sigma-Aldrich) followed by dehydration. Proteinase K digestion was then conducted at 37ºC for 38-45 min prior to post-fixation with 4% paraformaldehyde (Electron Microscopy Sciences, ProSciTech) in 1×PBS for 10 min. Acetylation treatment was carried out with 0.5% (v/v) acetic anhydride (Sigma) in 0.1 M triethanolamine hydrochloride (Sigma-Aldrich) for 10 min. Hybridization was performed overnight at 42ºC in hybridization buffer (50% [v/v] formamide, 2×SSC, 10% [v/v] dextran sulfate [Progen Biosciences], 1× Denhardt's solution [Sigma-Aldrich], and 1 µg/µL tRNA [Roche],], pH7.2-7.5) containing diluted DIG-labelled riboprobes. Slides were washed with 0.2×SSC at 42ºC before being treated in blocking solution (10% [v/v] Blocking Reagent [Roche] in 0.1 M maleic acid buffer). Immunological detection was performed using a 1:1250 dilution of anti-DIG antibody (anti-DIG-AP fab fragments150 U/200 µL, Roche,

11093274910) for 2 h followed by washing in TNM-50 detection buffer (100 mM Tris-HCl pH 9.5, 100 mM NaCl and 50 mM $MgCl_2$) for minimum 10 mins. Substrate (BM Purple [Roche], 1 mM levamisole [Sigma-Aldrich, L9756]) was applied and color development was monitored periodically until sufficient intensity was achieved. Reactions were stopped by incubating slides in TE twice for 5 min each. Slides were mounted with Crystal-Mount (Sigma-Aldrich) and observed using a Leica AS LMD Microscope and images were captured with a digital camera (SciTech). Images were processed with Photoshop Elements 2.0.

Subcellular Localization

Full length *Xat* minus the stop codon, XATΔSP, in which the signal peptide and the stop codon were removed, and the 63 bp of the *Xat* signal peptide only were cloned into the Golden Gate level zero CDS1ns acceptor pL0V-SC-41308 (Engler et al., 2014). All Golden Gate vector modules were kindly provided by S. Marillonnet. The internal BpiI restriction site was removed from the coding sequence of *Xat* using overlap PCR with the primers XAT-V214V-F and XAT-V214V-R (**Supplemental Table 2)**. The mCherry C-terminal module pL0M-C2-mCherry-15110 the Cauliflower mosaic virus (CaMV) 35S promotor module pL0M-PU-2x35S-TMV-3-51288 and the *nos* terminator module pL0M-T-Nos-1-41421 were combined with either the full length *XAT,* XATΔSP or the signal peptide only into the level 1 acceptor pL1V-R2-47811. Gene cassettes were then introduced into the level 2 binary vector pICSL4723 along with the 35S driven *hpt* gene to confer hygromycin resistance thus forming XAT-mCherry, XATΔSP-mCherry and SP-mCherry. A construct with an internal mCherry sequence introduced between the signal peptide of *Xat* and the remainder of the coding sequence was also generated. To achieve this, the *Xat* signal peptide fused to mCherry was PCR amplified from SP-mCherry using the primers mCHRYnoSTOP-BpiI-R and *Xat*-BpiI-F and cloned into pL0V-SC-41308. XATΔSP including the stop codon was amplified using the primers XatnoSP-BpiI-CT-F2 and XATSTP-BpiI-CT-R then cloned into the level zero CT acceptor pL0V-C2-15458. These constructs were combined into the vector pL1V-R2-47811 with pL0M-PU-2x35S-TMV-3-51288 and pL0M-T-Nos-1-41421 and the gene cassette cloned into binary vector pICSL4723.

Constructs were transformed into *Agrobacterium tumefaciens* (strain AGL1) via electroporation. 10 mL cultures were grown in half-salt LB media with kanamycin (50 µg/mL) and rifampicin (10

µg/mL) for two d at 28°C and 200 rpm. Bacteria were harvested by centrifugation at 3500 g for 10 min at room temperature and the pellet was resuspended in buffer containing 50 mM MES (pH 5.5), 50 mM $MgSO_4$, and 150 µM acetosyringone. Bacteria were diluted in this buffer to a final concentration of $O.D._{600}$ = 0.03 for each construct. Constructs were infiltrated singly or in pairs, as indicated in the figures, into expanding leaves of 4-6 week-old *Nicotiana benthamiana* plants. After two d, small regions of the transformed leaves were excised, mounted in water, and viewed using a 60x Apo TIRF objective on a Nikon TiE equipped with an Andor CSU-W1 spinning disc and a Borealis even illumination module. mCherry was excited at 561 nm and detected using a 610/40 filter, CFP and MDY-64 were excited at 445 nm and detected using a 470/40 filter, and FM1-43 was excited at 588 nm and detected using a 525/50 filter. Images were collected on an Andor iXon Ultra888 EM-CCD. Colocalization was assessed between the mCherry constructs described above and ER-CK (Nelson et al., 2007), the vacuole marker dye MDY-64 (Löfke et al., 2015) (ThermoFisher Y7536, diluted in water to 250nM from a 250µM stock in DMSO), or the plasma membrane dye FM1-43 (Bolte et al., 2004) (ThermoFisher T3163, diluted in water to 20 µM from a 20 mM stock in DMSO). For both dyes, small regions of the transformed leaves were excised, submerged in the dye solution, centrifuged at 600 g for 1 min to remove air and infiltrate with the dye, then rinsed twice in water and mounted as described above. Images were processed and line scan profiles were generated using Fiji.

Analysis of Gene Sequences

Multiple sequence alignment was performed using Clustal Omega (Sievers et al., 2011). Signal peptides were predicted using SignalP 4.0 software (Petersen et al., 2011). Phylogenetic tree construction was based on MUSCLE alignment of sequences from clade IV of the rice GDSL esterase/lipase (GELP) gene family (Chepyshko et al., 2012). The unrooted phylogenetic tree, which was constructed using the maximum likelihood method with 1,000 bootstrap replicates, includes XAT homologs from rice (OsGELP74), maize (GRMZM2G158205), barley (MLOC_58861), *Arabidopsis* (At3G16370) and tomato (Solyc03g121180), the cutin deficient 1 protein (CD1) from tomato (Solyc11g006250) and its *Arabidopsis* and rice homologs (At5G33370 and OsGELP40, respectively) and OsGELP12 from Clade I of the rice GELP family (Chepyshko et al., 2012).

Purification of Recombinant XAT

The coding region of *Xat*, excluding the first 63 bp, which encodes the predicted signal peptide, was cloned into the pHUE expression vector (Catanzariti et al., 2004) at the SacII and KpnI restriction sites using the primers sequences XAT-SacII-F, and XAT-KpnI-R (Supplemental Table 2). A XAT mutant (S37A) was generated by mutagenic PCR using overlapping primers, XATS37A-F and XATS37A-R (Supplemental Table 2), which contain one mismatch. Sequences were confirmed via Sanger sequencing. Cells of *Escherichia coli* (BL21 DE3 strain) containing the transformed constructs were cultured in LB media supplemented with ampicillin (50 µg/mL) and induced at an OD_{600} of 0.4 with the addition of 0.5 mM isopropyl thio-β-D-galactoside. Cultures were grown for a further 3.5 h at 28°C and harvested via centrifugation at 5000 g for 10 min. Cells were resuspended in lysis/binding buffer (50 mM Tris-Cl pH 8.0, 300 mM NaCl, 10 mM β-mercaptoethanol (BME), 30% [v/v] glycerol, 10 mM imidazole). Lysozyme (Sigma-Aldrich) was added to a concentration of 1 mg/mL and the bacterial solution was incubated on ice for 30 min. Cells were mechanically disrupted via homogenization using an EmulsiFlex-B15 (Avestin, Canada) and the soluble fraction was isolated via centrifugation (5000 g for 30 min). Protein was purified using Ni-NTA His-bind resin (Novagen, USA) per the manufacturer's instructions, except that all buffers used 50 mM Tris-Cl pH 8.0 and included 10% glycerol and 1 mM BME. Ultrafiltration was performed with storage buffer (50 mM Tris-Cl pH 8.0, 300 mM NaCl, 1 mM BME, 10% [v/v] glycerol) to remove imidazole and to concentrate the solution. The His-tagged ubiquitin fusion proteins were cleaved off in a 4 h incubation at 16°C with Usp2-cc protease (Catanzariti et al., 2004; Baker et al., 2005) at a 1:100 molar ratio. The final purified protein was recovered via passing through the Ni-NTA column which had been re-equilibrated with Storage buffer. All fractions were collected and analyzed a SDS-PAGE. Protein concentrations were measured using Bradford assays (Bradford, 1976).

Lipid Extraction from Wheat Flour

Lipid extractions from DM06.6*048 (a high lutein, zero-ester forming wheat line, University of Adelaide) flour were performed with an acidified version of the Bligh and Dyer method (Bahrami et al., 2014). Samples were dried under nitrogen gas stream and stored in 1 mL chloroform at -80°C in glass vials prior to use.

Enzymatic Assays

In vitro enzyme assays were performed in micelles following a modified protocol (Ilg et al., 2009). Lutein (40 μM) and the acyl-donor substrate (see below) were added to 50 μL of a 4% octyl-β-glucoside ethanolic solution containing 0.01% butylated hydroxytoluene. For assays with XAT(S37A) and assays determining optimal temperature, 60 μL out of the total 400 μL of lipids extracted from DM06.6*048 flour (see above) were used per replicate, which was estimated to be approximately 1.5 μg of total lipids (Bahrami et al., 2014). For assays to determine Michaelis-Menten enzyme kinetics, xanthophyll substrates and optimum pH, 5 mM of trilinolein (TAG) was used as the acyl donor. Samples were dried under N_2 gas to form a gel then resuspended in 100 μL incubation buffer (200 mM Tris-Cl pH 8.0, 2 mM tris(carboxyethyl)phosphine). Storage buffer (see purification of recombinant XAT) and 20 μg (unless otherwise indicated) of recombinant XAT were added to samples to a final assay volume of 200 μL. Samples were incubated at 37°C for 4 h (unless otherwise stated) and reactions were stopped with the addition of 400 μL acetone. Pigments were extracted via addition of 267 μl of ethyl acetate and 334 μL of water. Samples were centrifuged (14,000 g; 5 min) and the upper phase was transferred to a new tube, which was subsequently dried via vacuum centrifugation. Pigments were resuspended in 100 μL ethyl acetate and analyzed via HPLC. Kinetic data were fitted with Prism 5 software (GraphPad Software Inc, USA) using Michaelis-Menten non-linear regression.

Incubation buffer composition was altered for assays investigating the optimum pH of the enzyme with chemicals at 50 mM concentration used to maintain pH including sodium acetate (pH 4.0 and 5.0), sodium phosphate (pH 6.0 and 7.0), HEPES (pH 7.8), Tris-Cl (pH 8.0 and 9.0) and glycine-OH (pH 10.0). For assays investigating the acyl donor preference of the enzyme, lipid standards were purchased from Sigma: trilinolein a triacylglycerol (Sigma-Aldrich, T9517), 1,2-diglyceride (Sigma-Aldrich, D2135), 1,3-diglyceride (Sigma-Aldrich, D9508), monoglyceride (Sigma-Aldrich, M7640), L-α-phosphotidylcholine (Sigma-Aldrich, P0537) and L-α-lysophosphotidylcholine (Sigma-Aldrich, L5254). Each lipid was dissolved in chloroform and used at a 5 mM concentration in the final 200-μL assay. Chloroform was evaporated under N_2 gas prior to the addition of the incubation buffer and the enzyme (as above).

For assays investigating xanthophyll substrate preference, standards of zeaxanthin and β-cryptoxanthin were purchased from Sigma, suspended in ethanol and used at a 40 μM

concentration. Zeaxanthin used the octyl-β-glucoside micelles as above. Due to colloidal micelles not forming with β-cryptoxanthin, the activity of the enzyme was investigated using micelles formed with 150 μL of a 0.7% Triton X-100 and 1.6% Triton X-405 ethanolic detergent mixture as per previous protocol (Ilg et al., 2009). After the addition of 40 μM β-cryptoxanthin this mixture was dried under N_2 gas and resuspended in the incubation buffer (as above) to form micelles.

Saponification of Lutein Esters

Saponification of lutein ester fractions was performed as described (Galpaz et al., 2008). Carotenoids were partitioned against petroleum ether following the addition of NaCl to a final concentration of 1.9%. Pigments were dried under N_2 stream and analyzed via HPLC following resuspension in 100 μL ethyl acetate.

Analysis of Carotenoids from in vitro Enzyme Assays and Rice Embryogenic Calli

Extracted carotenoid pigments were analyzed via reverse-phase HPLC on a C-30 column (250 × 4.6 mm; YMC, Waters, Milford, USA) employing an Agilent 1110 Series HPLC (Agilent Technologies, Germany). Sample injections (45 μL) were separated at a flow rate of 1.5 mL min^{-1} with mobile phases of 0.1% methanolic ammonium acetate and 100% methyl tert-butyl ether. A gradient elution was performed as previously described (Alba et al., 2005).

Transformation of Rice Embryogenic Callus

Maize phytoene synthase 1 (GeneBank Accession: AAR08445) was PCR amplified from the Zm-PSY1-NT vector (Shumskaya et al., 2012; Gallagher et al., 2004) which was kindly provided by E. Wurtzel. *Pantoa agglomerans* phytoene desaturase (CrtI) (GenBank Accession: M38423.1) was fused in frame to the *Arabidopsis* SSU transit peptide from the small subunit of ribulose-1,5-bisphosphate carboxylase/oxygenase (Rubisco) and synthesized by GeneArt Gene Synthesis (ThermoFisher Scientific). *BETA-CAROTENE HYDROXYLASE 2* (AT5G52570) was cloned from *Arabidopsis thaliana* Col-0 cDNA. *Xat* was fused to the *Arabidopsis* SSU transit peptide sequence from Rubisco and generated by GeneArt Gene Synthesis (ThermoFisher Scientific). Multigene constructs were generated using Golden Gate modular cloning technology (Engler et al., 2014) with vector modules kindly provided by S. Marillonnet. Overlap PCR was used to remove internal

BpiI restriction sites from *Xat*, CrtI and *ZmPSY1* and an internal BsaI restriction site from *AtBCH2* (primers listed in Supplemental Table 1). Each gene was introduced into pL0V-SC-41308. Genes were combined with regulatory elements in level 1 vectors: *ZmPSY1* in pL1V-R2-47811; CrtI in pL1V-R3-47822, *AtBCH2* in pL1V-R4-47831 and SSU-XAT in pL1V-R5-47841. The ubiquitin 1 promotor from *Panicum virgatum* (*PvUbi*) (pL0M-PU-pPvUBI1-intron_15505) was used for expression of *ZmPSY1* and *AtBCH2*, the rice actin promotor (*OsActin*) (pL0M-PU-pOsAct1-intron-15216) was used for expression of SSU-CrtI, and the maize ubiquitin promotor (*ZmUbi*) (pL0M-PU-pZmUBI-intron1-15455) was used for expression of SSU-XAT. The *nos* terminator (NosT) module (pL0M-T-Nos-1-41421) was used for all genes. Gene cassettes were combined into the binary vector pICSL4723 along with the hygromycin phosphotrasferase gene (pL1M-R1-pOsAct1-HYG-tNOS-17100) to provide hygromycin resistance.

Constructs were introduced into *Agrobacterium tumefaciens* strain AGL1 via electroporation and transformed into rice embryogenic callus following the protocol described by Hiei and Komari (2006). Transformed calli were grown in the dark at 25°C and subcultured every two weeks on N6D media (3% [w/v] sucrose, 3.98 g L^{-1} CHU[N6] basal mixture [Austratec], 0.1 g L^{-1} myo-inositol, 0.3 g L^{-1} casamino acids, 25 mM L-proline, 2 mg L^{-1} glycine, 1 mg L^{-1} thiamine, 0.5 mg L^{-1} pyridoxine, 0.5 mg L^{-1} nicotinic acid, 0.2 mg L^{-1} 2,4-dichlorophenoxyacetic acid, 150 mg L^{-1} timentin, 0.4% [w/v] gellan gum, pH 5.8 adjusted with 1 N KOH) supplemented with 35 mg L^{-1} hygromycin B until sufficient callus material for carotenoid analysis via HPLC was generated. HPLC analysis was performed using the same method as used for analysis of the in vitro enzymatic assays.

Accession numbers

Sequence data for the wheat gene *Xat* can be found in the EMBL/GenBank data libraries under accession number MN233788. Accession numbers of *Xat* homologs used for this study are as follows: Barley (*Hordeum vulgare*, MLOC 58861), maize (*Zea mays*, GRMZM2G158205), rice (*Oryza sativa*, Os06g148200), *Arabidopsis thaliana* (At3g16370), tomato (*Solanum lycopersicum*, Solyc03g121180) and EstA from *Pseudomonas aeruginosa* (PDB accession number 3KVN). Accession numbers of sequences for construction of the rice GDSL phylogenetic tree are provided in Supplemental File 1.

Table 1: Concentration of Esterified Lutein in Durum Wheat Disomic Substitution Lines

Variety	*trans*-lutein (µg/g)	*cis*-isomer (µg/g)	Mono-esters (µg/g)	Di-esters (µg/g)	Total *trans*-lutein (µg/g)	Lutein esters (%)
Langdon	1.89 ± 0.07	0.55 ± 0.01	ND	ND	1.89^{a} ± 0.07	ND
7D(7A)	0.68 ± 0.02	0.18 ± 0.03	0.64 ± 0.04	1.02 ± 0.05	2.34^{b} ± 0.11	69.93 ± 1.96
7D(7B)	0.85 ± 0.11	0.41 ± 0.08	0.41 ± 0.08	1.30 ± 0.20	2.56^{b} ± 0.36	66.60 ± 1.05

Concentration of free lutein (*cis* and *trans* isomers), lutein mono- and lutein di-esters in grain of the durum wheat cultivar Langdon and two disomic substitution lines in which a pair of 7D chromosomes from Chinese Spring wheat has been substituted for the 7A or 7B chromosome pair of Langdon. For total *trans*-lutein content, significant differences are indicated ^{a,b} (ANOVA: $p<0.05$, LSD = 0.34 for n = 3 biological replicates). Lutein esters (mono- and di-) are also reported as the percentage of total *trans*-lutein. All other carotenoids, including β-carotene and α-carotene, were at trace levels. ND, not detected.

Table 2: Mutations in *Xat* in a Gladius Bread Wheat TILLING Population

M_2 family	Nucleotide change	Amino acid change	Mutation type	Proportion of lutein esters normalised to Gladius
Gladius			Wildtype	1.0 ± 0.01 [a]
Ga51	G511A		Splice	ND
Ga112	C601T	Q131stop	Truncation	ND
Ga236	C760T	Q184stop	Truncation	ND
Ga64	C979T	P219L	Missense	ND
ga243	G164A	D40N	Missense	ND
ga483	G164A	D40N	Missense	ND
ga12	G440A	G101E	Missense	0.65 ± 0.08 [b]
ga334	C428T	P97L	Missense	0.61 ± 0.05 [b]

Detection and quantification of lutein esters in grain harvested from M3 plants homozygous for *Xat* mutant alleles. *Xat* mutant alleles were identified from 768 TILLING lines of an EMS-mutagenized bread wheat (cultivar Gladius) population. For samples where lutein esters were detected, data show the proportion of esterified lutein normalized to the wildtype, Gladius ± SEM for n = 4-9 biological replicates. The Gladius cultivar accumulates 59 ± 1% lutein esters from the total carotenoid pool (n = 9). The remainder of the carotenoids present in Gladius grain is free lutein, present in either its *cis*- or all-*trans* isomers. Statistically significant differences are indicated by [a, b] ($p<0.05$). ND, not detected.

Table 3: XAT Acyl-Donor Substrate Preference

Lipid Substrate	Relative activity (%)
Triglycerides	100 ± 2.9 [a]
1,2-Diglycerides	31 ± 18 [b]
Lysophosphotidylcholine	13.6 ± 1.0 [b]
Free fatty acids	9.3 ± 1.8 [b]
1,3-Diglycerides	3.5 ± 0.2 [b]
Monoglycerides	1.8 ± 0.7 [b]
Phosphotidylcholine	ND

In vitro enzyme assays were performed with 20 μg of recombinant XAT and 5 mM of acyl-donor substrate. Assays were performed at 37°C and pH 8.0 for 4 h in a final assay volume of 200 μL. Data show activity ± SE relative to trilinolein (Triglyceride) for n=3 biological replicates from one representative experiment. Experiment was performed 2 times, with similar results. Statistically significant differences are indicated by a, b ($p<0.05$). ND. , not detected.

Table 4: Kinetic Parameters of Recombinant XAT

Enzyme	Reaction	Substrate	Km (μM)	Reference
XAT	Transesterification	Lutein (xanthophyll)	60.2 ± 7.6[a]	This work
XAT	Transesterification	Trilinolein (TAG)	50.6 ± 27[a]	This work
XAT	Hydrolysis - lipase	*p*-nitrophenyl palmitate	160 ± 67[b]†	This work
XAT	Hydrolysis - esterase	*p*-nitrophenyl acetate	474 ± 94[a]	This work
CD1	Transesterification	2-mono-(10,16-dihydroxyhexadecanoyl) glycerol	925 ± 98	(Yeats et al., 2014)
BS1	Hydrolysis	2,3,4-tri-*O*-acetyl-methyl β-D-xylopyranoside	4400 ± 780	(Zhang et al., 2017)

K_m was calculated using Michaelis-Menten plots using 20 μg recombinant protein for lutein, 52 μg for the TAG substrate and 10 μg of XAT for both the nitrophenyl ester substrates. Kinetic data previously calculated for reactions catalyzed by other plant GDSL esterase/lipases, tomato CD1 and rice BS1, have also been included. CD1 is part of the same phylogenetic clade as XAT, Clade IV as designated by (Chepyshko et al., 2012), (see Figure 2), whereas BS1 is from Clade I of the GELP family. † denotes apparent K_m value as reaction preceded too fast to observe kinetics at low concentration of substrate.

Supplemental Data

Supplemental Figure 1. SDS-PAGE Analysis of XAT and Mutated XAT (S37A) Recombinant Proteins.

Supplemental Figure 2. Determination of XAT Kinetic Parameters.

Supplemental Figure 3. Colocalization of XAT mCherry Fusion Proteins and Controls with an Endoplasmic Reticulum Marker in *N. benthamiana* Leaves.

Supplemental Figure 4. Colocalization of XAT mCherry Fusion Proteins and Controls with a Plasma Membrane Dye in *N. benthamiana* Leaves.

Supplemental Figure 5. XAT has Esterase and Lipase Activity with *p*-nitrophenyl Esters.

Supplemental Figure 6. Constitutive *Xat* Overexpression Does Not Affect Total Carotenoid Accumulation.

Supplemental Table 1. Effect of pH on XAT Activity.

Supplemental Table 2. Primer Sequences Used in this Study.

Supplemental File 1. Accession numbers for sequences used in GDSL phylogenetic tree.

Supplemental File 2. Alignment used for the phylogenetic analysis.

Supplemental File 3. ANOVA Tables.

ACKNOWLEDGMENTS

We acknowledge Riya Kuruvilla for help with rice transformation and tissue culture, Robert Asenstorfer for assistance in lipid partitioning, Ian Dundas for providing seed of Langdon and the Langdon disomic substitution lines, Ursula Langridge for providing developing grains of Gladius, Gwen Mayo and Adelaide Microscopy, an AMMF facility at the University of Adelaide, for microscopy advice and services and the International Wheat Genome Sequencing Consortium (http://www.wheatgenome.org) for providing prepublication access to IWGSC RefSeq v1.0. Live cell imaging was conducted using equipment from the University of Melbourne Advanced Microscopy Facility and the Biological Optical Microscopy Platform. This research was funded by the Grains Research and Development Corporation (UA00102), ARC Centre of Excellence in Plant Energy Biology (CE140100008) and the ARC Centre of Excellence in Translational Photosynthesis (CE1401000015). HEM is supported by an ARC DECRA (DE170100054). KXC is funded by a Postdoctoral Fellowship from the Research Foundation – Flanders (FWO; 12N4818N). JLW was supported by an Australian Research Training Program (RTP) Scholarship.

AUTHOR CONTRIBUTIONS

JLW: design, execution and analysis of experiments and wrote the manuscript; ML: design, execution and analysis of experiments; RPM, KXC and DM: contributed to the design of biochemical analyses; HEMcF: subcellular localization; ME and RTF: rice transgenesis; CD, KJC and PS: wheat genetics; JLW, DEM and BJP: overall design, interpretation and writing, with input from all coauthors.

REFERENCES

Abdel-Aal, E.S.M. and Rabalski, I. (2015). Composition of lutein ester regioisomers in marigold flower, dietary supplement, and herbal tea. J. Agric. Food Chem. **63**: 9740–9746.

Ahmad, F.T., Asenstorfer, R.E., Soriano, I.R., and Mares, D.J. (2013). Effect of temperature on lutein esterification and lutein stability in wheat grain. J. Cereal Sci. **58**: 408–413.

Ahmad, F.T., Mather, D.E., Law, H.-Y., Li, M., Yousif, S.A.-J., Chalmers, K.J., Asenstorfer, R.E., and Mares, D.J. (2015). Genetic control of lutein esterification in wheat (\emph{Triticum aestivum} L.) grain. J. Cereal Sci. **64**: 109–115.

Akoh, C.C., Lee, G.C., Liaw, Y.C., Huang, T.H., and Shaw, J.F. (2004). GDSL family of serine esterases/lipases. Prog. Lipid Res. **43**: 534–552.

Alba, R., Payton, P., Fei, Z., McQuinn, R., Debbie, P., Martin, G.B., Tanksley, S.D., and Giovannoni, J.J. (2005). Transcriptome and selected metabolite analyses reveal multiple points of ethylene control during tomato fruit development. Plant Cell **17**: 2954–65.

Ariizumi, T. et al. (2014). Identification of the carotenoid modifying gene \emph{PALE YELLOW PETAL 1} as an essential factor in xanthophyll esterification and yellow flower pigmentation in tomato (\emph{Solanum lycopersicum}). Plant J. **79**: 453–465.

Auldridge, M.E., Block, A., Vogel, J.T., Dabney-Smith, C., Mila, I., Bouzayen, M., Magallanes-Lundback, M., DellaPenna, D., McCarty, D.R., and Klee, H.J. (2006). Characterization of three members of the Arabidopsis carotenoid cleavage dioxygenase family demonstrates the divergent roles of this multifunctional enzyme family. Plant J. **45**: 982–993.

Bahrami, N., Yonekura, L., Linforth, R., Carvalho da Silva, M., Hill, S., Penson, S., Chope, G., and Fisk, I.D. (2014). Comparison of ambient solvent extraction methods for the analysis of fatty acids in non-starch lipids of flour and starch. J. Sci. Food Agric. **94**: 415–423.

Bai, C., Rivera, S.M., Medina, V., Alves, R., Vilaprinyo, E., Sorribas, A., Canela, R., Capell, T., Sandmann, G., Christou, P., and Zhu, C. (2014). An \emph{in vitro} system for the rapid functional characterization of genes involved in carotenoid biosynthesis and accumulation. Plant J. **77**: 464–475.

Bailly, C. (2004). Active oxygen species and antioxidants in seed biology. Seed Sci. Res. **14**: 93–107.

Baker, R.T., Catanzariti, A.M., Karunasekara, Y., Soboleva, T.A., Sharwood, R., Whitney, S., and Board, P.G. (2005). Using deubiquitylating enzymes as research tools. Methods Enzymol. **398**: 540–554.

Bartley, G.E., Viitanen, P. V., Pecker, I., Chamovitz, D., Hirschberg, J., and Scolnik, P.A. (1991). Molecular cloning and expression in photosynthetic bacteria of a soybean cDNA coding for phytoene desaturase, an enzyme of the carotenoid biosynthesis pathway. Proc. Natl. Acad. Sci. U. S. A. **88**: 6532–6536.

Berry, H.M., Rickett, D. V, Baxter, C., Enfissi, E.M.A., and Fraser, P.D. (2019). Carotenoid biosynthesis and sequestration in red chilli pepper fruit and its impact on colour intensity traits. J. Exp. Bot. **70**: 1–14.

Beyene, G. et al. (2018). Provitamin A biofortification of cassava enhances shelf life but reduces dry matter content of storage roots due to altered carbon partitioning into starch. Plant Biotechnol. J. **16**: 1186–1200.

Biacs, P. a., Daood, H.G., Pavisa, A., and Hajdu, F. (1989). Studies on the carotenoid pigments of paprika (\emph{Capsicum annuum} L.var Sz-20). J. Agric. Food Chem. **37**: 350–353.

Bolte, S., Talbot, C., Boutte, Y., Catrice, O., Read, N.D., and Satiat-Jeunemaitre, B. (2004). FM-dyes as experimental probes for dissecting vesicle trafficking in living plant cells. J. Microsc. **214**: 159–173.

Boussiba, S. (2000). Carotenogenesis in the green alga \emph{Haematococcus pluvialis} : Cellular physiology and stress response. Physiol. Plant. **108**: 111–117.

Bradford, M.M. (1976). A rapid and sensitive method for the quantitation of microgram quantities of protein utilizing the principle of protein-dye binding. Anal. Biochem. **72**: 248–254.

Breithaupt, D.E. and Bamedi, A. (2002). Carotenoids and carotenoid esters in potatoes (\emph{Solanum tuberosum} L.): New insights into an ancient vegetable. J. Agric. Food Chem. **50**: 7175–7181.

Breithaupt, D.E., Wirt, U., and Bamedi, A. (2002). Differentiation between lutein monoester regioisomers and detection of lutein diesters from marigold flowers (\emph{Tagetes erecta} L.) and several fruits by liquid chromatography-mass spectrometry. J. Agric. Food Chem. **50**: 66–70.

Catanzariti, A.-M., Soboleva, T. a, Jans, D. a, Board, P.G., and Baker, R.T. (2004). An efficient system for high-level expression and easy purification of authentic recombinant proteins. Protein Sci. **13**: 1331–1339.

Chen, G., Wang, B., Han, D., Sommerfeld, M., Lu, Y., Chen, F., and Hu, Q. (2015). Molecular mechanisms of the coordination between astaxanthin and fatty acid biosynthesis in \emph{Haematococcus pluvialis} (Chlorophyceae). Plant J. **81**: 95–107.

Chen, Y., Li, F., and Wurtzel, E.T. (2010). Isolation and characterization of the \emph{Z-ISO} gene encoding a

missing component of carotenoid biosynthesis in plants. Plant Physiol. **153**: 66–79.
Chepyshko, H., Lai, C.-P., Huang, L.-M., Liu, J.-H., and Shaw, J.-F. (2012). Multifunctionality and diversity of GDSL esterase/lipase gene family in rice (\emph{Oryza sativa} L. \emph{japonica}) genome: new insights from bioinformatics analysis. BMC Genomics **13**: 309.
Cho, W.K., Chen, X.Y., Chu, H., Rim, Y., Kim, S., Kim, S.T., Kim, S.W., Park, Z.Y., and Kim, J.Y. (2009). Proteomic analysis of the secretome of rice calli. Physiol. Plant. **135**: 331–341.
Clauss, K., Baumert, A., Nimtz, M., Milkowski, C., and Strack, D. (2008). Role of a GDSL lipase-like protein as sinapine esterase in \emph{Brassicaceae}. Plant J. **53**: 802–813.
Concepcion, M.R. et al. (2018). A global perspective on carotenoids: Metabolism, biotechnology, and benefits for nutrition and health. Prog. Lipid Res. **70**: 62–93.
Deruère, J., Römer, S., D'Harlingue, A., Backhaus, R. a, Kuntz, M., and Camara, B. (1994). Fibril assembly and carotenoid overaccumulation in chromoplasts: a model for supramolecular lipoprotein structures. Plant Cell **6**: 119–133.
Domínguez, F. and Cejudo, F.J. (2014). Programmed cell death (PCD): an essential process of cereal seed development and germination. Front. Plant Sci. **5**: 366.
Dong, C., Dalton-Morgan, J., Vincent, K., and Sharp, P. (2009). A Modified TILLING Method for Wheat Breeding. Plant Genome J. **2**: 39.
Dong, H., Deng, Y., Mu, J., Lu, Q., Wang, Y., Xu, Y., Chu, C., Chong, K., Lu, C., and Zuo, J. (2007). The Arabidopsis *Spontaneous Cell Death1* gene, encoding a ζ-carotene desaturase essential for carotenoid biosynthesis, is involved in chloroplast development, photoprotection and retrograde signalling. Cell Res. **17**: 458–470.
Enfissi, E.M.A., Nogueira, M., D'Ambrosio, C., Stigliani, A.L., Giorio, G., Misawa, N., and Fraser, P.D. (2019). The road to astaxanthin production in tomato fruit reveals plastid and metabolic adaptation resulting in an unintended high lycopene genotype with delayed over-ripening properties. Plant Biotechnol. J.: 1–13.
Engler, C., Youles, M., Gruetzner, R., Ehnert, T.M., Werner, S., Jones, J.D.G., Patron, N.J., and Marillonnet, S. (2014). A Golden Gate modular cloning toolbox for plants. ACS Synth. Biol. **3**: 839–843.
Fernandez-Orozco, R., Gallardo-Guerrero, L., and Hornero-Méndez, D. (2013). Carotenoid profiling in tubers of different potato (\emph{Solanum} sp) cultivars: Accumulation of carotenoids mediated by xanthophyll esterification. Food Chem. **141**: 2864–2872.
Fraser, P.D., Misawa, N., Linden, H., Yamano, S., Kobayashi, K., and Sandmann, G. (1992). Expression in *Escherichia coli*, purification, and reactivation of the recombinant *Erwinia uredovora* phytoene desaturase. J. Biol. Chem. **267**: 19891–19895.
Fu, H., Xie, B., Fan, G., Ma, S., Zhu, X., and Pan, S. (2010). Effect of esterification with fatty acid of beta-cryptoxanthin on its thermal stability and antioxidant activity by chemiluminescence method. Food Chem. **122**: 602–609.
Gallagher, C.E., Matthews, P.D., Li, F., and Wurtzel, E.T. (2004). Gene duplication in the carotenoid biosynthetic pathway preceded evolution of the grasses. Plant Physiol. **135**: 1776–83.
Galpaz, N., Wang, Q., Menda, N., Zamir, D., and Hirschberg, J. (2008). Abscisic acid deficiency in the tomato mutant \emph{high-pigment 3} leading to increased plastid number and higher fruit lycopene content. Plant J. **53**: 717–730.
García-de Blas, E., Mateo, R., Viñuela, J., Pérez-Rodríguez, L., and Alonso-Alvarez, C. (2013). Free and esterified carotenoids in ornaments of an avian species: the relationship to color expression and sources of variability. Physiol. Biochem. Zool. **86**: 483–98.
Giordano, E. and Quadro, L. (2018). Lutein, zeaxanthin and mammalian development: Metabolism, functions and implications for health. Arch. Biochem. Biophys. **647**: 33–40.
Harjes, C.E., Rocheford, T.R., Bai, L., Brutnell, T.P., Kandianis, C.B., Sowinski, S.G., Stapleton, A.E., Vallabhaneni, R., Williams, M., Wurtzel, E.T., Yan, J., and Buckler, E.S. (2008). Natural genetic variation in lycopene epsilon cyclase tapped for maize biofortification. Science **319**: 330–333.
Hiei, Y. and Komari, T. (2006). Improved protocols for transformation of indica rice mediated by *Agrobacterium tumefaciens*. Plant Cell. Tissue Organ Cult. **85**: 271–283.
Hong, J.K., Choi, H.W., Hwang, I.S., Kim, D.S., Kim, N.H., Choi, D.S., Kim, Y.J., and Hwang, B.K. (2008). Function of a novel GDSL-type pepper lipase gene, *CaGLIP1*, in disease susceptibility and abiotic stress tolerance. Planta **227**: 539–558.
Howitt, C. a. and Pogson, B.J. (2006). Carotenoid accumulation and function in seeds and non-green tissues. Plant, Cell Environ. **29**: 435–445.
Howitt, C.A., Cavanagh, C.R., Bowerman, A.F., Cazzonelli, C., Rampling, L., Mimica, J.L., and Pogson, B.J.

(2009). Alternative splicing, activation of cryptic exons and amino acid substitutions in carotenoid biosynthetic genes are associated with lutein accumulation in wheat endosperm. Funct. Integr. Genomics **9**: 363–376.

Huang, L.-M., Lai, C.-P., Chen, L.-F.O., Chan, M.-T., and Shaw, J.-F. (2015). Arabidopsis SFAR4 is a novel GDSL-type esterase involved in fatty acid degradation and glucose tolerance. Bot. Stud. **56**: 33.

Huang, Y.T., Liaw, Y.C., Gorbatyuk, V.Y., and Huang, T.H. (2001). Backbone dynamics of \emph{Escherichia coli} thioesterase/protease I: evidence of a flexible active-site environment for a serine protease. J. Mol. Biol. **307**: 1075–1090.

Ilg, A., Beyer, P., and Al-Babili, S. (2009). Characterization of the rice carotenoid cleavage dioxygenase 1 reveals a novel route for geranial biosynthesis. FEBS J. **276**: 736–747.

Johnson, E.J. (2014). Role of lutein and zeaxanthin in visual and cognitive function throughout the lifespan. Nutr. Rev. **72**: 605–612.

Joppa, L.R. and Williams, N.D. (1988). Langdon durum disomic substitution lines and aneuploid analysis in tetraploid wheat. Genome **30**: 222–228.

Kaneko, S., Nagamine, T., and Yamada, T. (1995). Esterification of endosperm lutein with fatty acids during the storage of wheat seeds. Biosci. Biotechnol. Biochem. **59**: 1–4.

Kaneko, S. and Oyanagi, A. (1995). Varietal Differences in the Rate of Esterification of Endosperm Lutein during the Storage of Wheat Seeds. Biosci. Biotechnol. Biochem. **59**: 2312–2313.

Kijlstra, A., Tian, Y., Kelly, E.R., and Berendschot, T.T.J.M. (2012). Lutein: More than just a filter for blue light. Prog. Retin. Eye Res. **31**: 303–315.

Kikuta, Y., Ueda, H., Takahashi, M., Mitsumori, T., Yamada, G., Sakamori, K., Takeda, K., Furutani, S., Nakayama, K., Katsuda, Y., Hatanaka, A., and Matsuda, K. (2012). Identification and characterization of a GDSL lipase-like protein that catalyzes the ester-forming reaction for pyrethrin biosynthesis in \emph{Tanacetum cinerariifolium} - A new target for plant protection. Plant J. **71**: 183–193.

Kim, K.J., Lim, J.H., Kim, M.J., Kim, T., Chung, H.M., and Paek, K.H. (2008). GDSL-lipase1 (*CaGL1*) contributes to wound stress resistance by modulation of CaPR-4 expression in hot pepper. Biochem. Biophys. Res. Commun. **374**: 693–698.

Lee, D.S., Kim, B.K., Kwon, S.J., Jin, H.C., and Park, O.K. (2009). *Arabidopsis* GDSL lipase 2 plays a role in pathogen defense via negative regulation of auxin signaling. Biochem. Biophys. Res. Commun. **379**: 1038–1042.

Lee, L.-C., Lee, Y.-L., Leu, R.-J., and Shaw, J.-F. (2006). Functional role of catalytic triad and oxyanion hole-forming residues on enzyme activity of \emph{Escherichia coli} thioesterase I/protease I/phospholipase L\textsubscript{1}. Biochem. J. **397**: 69–76.

Lee, Y.L., Chen, J.C., and Shaw, J.F. (1997). The thioesterase I of \emph{Escherichia coli} has arylesterase activity and shows stereospecificity for protease substrates. Biochem. Biophys. Res. Commun. **231**: 452–456.

Li, C. et al. (2017). A GDSL-motif esterase/acyltransferase/lipase is responsible for leaf water retention in barley. Plant Direct **1**: e00025.

Li, W., Gao, Y., Zhao, J., and Qi, W. (2007). Phenolic, flavonoid, and lutein ester content and antioxidant activity of 11 cultivars of Chinese marigold. J. Agric. Food Chem. **55**: 8478–8484.

Löfke, C., Dünser, K., Scheming, D., and Kleine-Vehn, J. (2015). Auxin regulates SNARE-dependent vacuolar morphology restricting cell size. Elife **2015**: 1–16.

Mattera, M.G., Cabrera, A., Hornero-Méndez, D., and Atienza, S.G. (2015). Lutein esterification in wheat endosperm is controlled by the homoeologous group 7, and is increased by the simultaneous presence of chromosomes 7D and 7H^{ch} from \emph{Hordeum chilense}. Crop Pasture Sci. **66**: 912–921.

Mattera, M.G., Hornero-Méndez, D., and Atienza, S.G. (2017). Lutein ester profile in wheat and tritordeum can be modulated by temperature: Evidences for regioselectivity and fatty acid preferential of enzymes encoded by genes on chromosomes 7D and 7H^{ch}. Food Chem. **219**: 199–206.

Mellado-Ortega, E., Atienza, S.G., and Hornero-Méndez, D. (2015). Carotenoid evolution during postharvest storage of durum wheat (\emph{Triticum turgidum} conv. \emph{durum}) and tritordeum (\emph{$\times$Tritordeum} Ascherson et Graebner) grains. J. Cereal Sci. **62**: 134–142.

Mellado-Ortega, E., Atienza, S.G., and Hornero-Méndez, D. (2016). Carotenoid evolution during short-storage period of durum wheat (\emph{Triticum turgidum} conv. \emph{durum}) and tritordeum (\emph{$\times$Tritordeum} Ascherson et Graebner) whole-grain flours. J. Cereal Sci. **192**: 714–723.

Mellado-Ortega, E. and Hornero-Méndez, D. (2015). Carotenoid profiling of \emph{Hordeum chilense} grains: The parental proof for the origin of the high carotenoid content and esterification pattern of tritordeum. J. Cereal Sci. **62**: 15–21.

Mellado-Ortega, E. and Hornero-Méndez, D. (2017). Lutein Esterification in Wheat Flour Increases the Carotenoid

Retention and Is Induced by Storage Temperatures. Foods **6**: 111.
Mercadante, A.Z., Rodrigues, D.B., Petry, F.C., and Mariutti, L.R.B. (2017). Carotenoid esters in foods - A review and practical directions on analysis and occurrence. Food Res. Int. **99**: 830–850.
Mertz, C., Brat, P., Caris-Veyrat, C., and Gunata, Z. (2010). Characterization and thermal lability of carotenoids and vitamin C of tamarillo fruit (\emph{Solanum betaceum} Cav.). Food Chem. **119**: 653–659.
Millar, A.H., Carrie, C., Pogson, B., and Whelan, J. (2009). Exploring the function-location nexus: using multiple lines of evidence in defining the subcellular location of plant Pproteins. Plant Cell Online **21**: 1625–1631.
Minguez-Mosquera, M.I. and Hornero-Mendez, D. (1994). Changes in carotenoid esterification during the fruit ripening of \emph{Capsicum annuum} Cv. Bola. J. Agric. Food Chem. **42**: 640–644.
Møller, I.S., Gilliham, M., Jha, D., Mayo, G.M., Roy, S.J., Coates, J.C., Haseloff, J., and Tester, M. (2009). Shoot Na+ exclusion and increased salinity tolerance engineered by cell type-specific alteration of Na+ transport in Arabidopsis. Plant Cell **21**: 2163–2178.
Morrison, W.R. (1978). Wheat Lipids Composition. Cereal Chem. **55**: 548–558.
Ndolo, V.U. and Beta, T. (2013). Distribution of carotenoids in endosperm, germ, and aleurone fractions of cereal grain kernels. Food Chem. **139**: 663–671.
Nelson, B.K., Cai, X., and Nebenführ, A. (2007). A multicolored set of in vivo organelle markers for co-localization studies in Arabidopsis and other plants. Plant J. **51**: 1126–1136.
Nisar, N., Li, L., Lu, S., Khin, N.C., and Pogson, B.J. (2015). Carotenoid metabolism in plants. Mol. Plant **8**: 68–82.
Oh, I.S., Park, A.R., Bae, M.S., Kwon, S.J., Kim, Y.S., Lee, J.E., Kang, N.Y., Lee, S., Cheong, H., and Park, O.K. (2005). Secretome Analysis Reveals an Arabidopsis Lipase Involved in Defense against \emph{Alternaria brassicicola}. Plant Cell **17**: 2832–2847.
Park, H., Kreunen, S.S., Cuttriss, A.J., DellaPenna, D., and Pogson, B.J. (2002). Identification of the Carotenoid Isomerase Provides Insight into Carotenoid Biosynthesis, Prolamellar Body Formation, and Photomorphogenesis. Plant Cell Online **14**: 321–332.
Paznocht, L., Kotíková, Z., Šulc, M., Lachman, J., Orsák, M., Eliášová, M., and Martinek, P. (2018). Free and esterified carotenoids in pigmented wheat, tritordeum and barley grains. Food Chem. **240**: 670–678.
Petersen, T.N., Brunak, S., von Heijne, G., and Nielsen, H. (2011). SignalP 4.0: discriminating signal peptides from transmembrane regions. Nat. Methods **8**: 785–6.
Ramírez-González, R.H. et al. (2018). The transcriptional landscape of polyploid wheat. Science (80-.). **361**.
Ríos, J.J., Xavier, A.A.O., Díaz-Salido, E., Arenilla-Vélez, I., Jarén-Galán, M., Garrido-Fernández, J., Aguayo-Maldonado, J., and Pérez-Gálvez, A. (2017). Xanthophyll esters are found in human colostrum. Mol. Nutr. Food Res. **201700296**: 1–9.
Rodriguez, K., Perales, M., Snipes, S., Yadav, R.K., Diaz-Mendoza, M., and Reddy, G.V. (2016). DNA-dependent homodimerization, sub-cellular partitioning, and protein destabilization control WUSCHEL levels and spatial patterning. Proc. Natl. Acad. Sci. **113**: E6307–E6315.
Roepke, J., Salim, V., Wu, M., Thamm, A.M.K., Murata, J., Ploss, K., Boland, W., and De Luca, V. (2010). Vinca drug components accumulate exclusively in leaf exudates of Madagascar periwinkle. Proc. Natl. Acad. Sci. **107**: 15287–15292.
Sanger, F., Nicklen, S., and Coulson, A.R. (1977). DNA sequencing with chain-terminating inhibitors. Proc. Natl. Acad. Sci. **74**: 5463–5467.
Sattler, S.E., Gilliland, L.U., Magallanes-Lundback, M., Pollard, M., and DellaPenna, D. (2004). Vitamin E Is Essential for Seed Longevity and for Preventing Lipid Peroxidation during Germination. Plant Cell **16**: 1419–1432.
Schweiggert, U., Kurz, C., Schieber, A., and Carle, R. (2007). Effects of processing and storage on the stability of free and esterified carotenoids of red peppers (\emph{Capsicum annuum} L.) and hot chilli peppers (\emph{Capsicum frutescens} L.). Eur. Food Res. Technol. **225**: 261–270.
Sharp, P. and Dong, C. (2014). TILLING for plant breeding. In Crop Breeding: Methods and Protocols (Humana Press: New York), pp. 155–165.
Shumskaya, M., Bradbury, L.M.T., Monaco, R.R., and Wurtzel, E.T. (2012). Plastid Localization of the Key Carotenoid Enzyme Phytoene Synthase Is Altered by Isozyme, Allelic Variation, and Activity. Plant Cell **24**: 3725–3741.
Shumskaya, M. and Wurtzel, E.T. (2013). The carotenoid biosynthetic pathway: thinking in all dimensions. Plant Sci. **208**: 58–63.
Sievers, F., Wilm, A., Dineen, D., Gibson, T.J., Karplus, K., Li, W., Lopez, R., McWilliam, H., Remmert, M., Söding, J., Thompson, J.D., and Higgins, D.G. (2011). Fast, scalable generation of high-quality protein

multiple sequence alignments using Clustal Omega. Mol. Syst. Biol. **7**: 539.

Subagio, A. and Morita, N. (2003). Prooxidant activity of lutein and its dimyristate esters in corn triacylglyceride. Food Chem. **81**: 97–102.

Subagio, A., Wakaki, H., and Morita, N. (1999). Stability of lutein and its myristate esters. Biosci. Biotechnol. Biochem. **63**: 1784–1786.

Sun, T., Yuan, H., Cao, H., Yazdani, M., Tadmor, Y., and Li, L. (2018). Carotenoid Metabolism in Plants: The Role of Plastids. Mol. Plant **11**: 58–74.

Takahashi, K., Shimada, T., Kondo, M., Tamai, A., Mori, M., Nishimura, M., and Hara-Nishimura, I. (2010). Ectopic expression of an esterase, which is a candidate for the unidentified plant cutinase, causes cuticular defects in \emph{Arabidopsis thaliana}. Plant Cell Physiol. **51**: 123–131.

Tanaka, H., Shimizu, R., and Tsujimoto, H. (2005). Genetical analysis of contribution of low-molecular-weight glutenin subunits to dough strength in common wheat (\emph{Triticum aestivum} L .). Euphytica **141**: 157–162.

Tanaka, T., Shnimizu, M., and Moriwaki, H. (2012). Cancer chemoprevention by carotenoids. Molecules **17**: 3202–3242.

Tapiero, H., Townsend, D.M., and Tew, K.D. (2004). The role of carotenoids in the prevention of human pathologies. Biomed. Pharmacother. **58**: 100–110.

Updegraff, E.P., Zhao, F., and Preuss, D. (2009). The extracellular lipase \emph{EXL4} is required for efficient hydration of Arabidopsis pollen. Sex. Plant Reprod. **22**: 197–204.

Vallabhaneni, R., Gallagher, C.E., Licciardello, N., Cuttriss, A.J., Quinlan, R.F., and Wurtzel, E.T. (2009). Metabolite sorting of a germplasm collection reveals the \emph{Hydroxylase3} locus as a new target for maize provitamin A biofortification. Plant Physiol. **151**: 1635–1645.

Volokita, M., Rosilio-Brami, T., Rivkin, N., and Zik, M. (2011). Combining comparative sequence and genomic data to ascertain phylogenetic relationships and explore the evolution of the large GDSL-lipase family in land plants. Mol. Biol. Evol. **28**: 551–565.

Wade, N., Goulter, K.C., Wilson, K.J., Hall, M.R., and Degnan, B.M. (2005). Esterified astaxanthin levels in lobster epithelia correlate with shell colour intensity: Potential role in crustacean shell colour formation. Comp. Biochem. Physiol. - B Biochem. Mol. Biol. **141**: 307–313.

Wingerath, T., Sies, H., and Stahl, W. (1998). Xanthophyll esters in human skin. Arch. Biochem. Biophys. **355**: 271–4.

Yabuzaki, J. (2017). Carotenoids Database: Structures, chemical fingerprints and distribution among organisms. Database **2017**: 1–11.

Yeats, T.H., Huang, W., Chatterjee, S., Viart, H.M.F., Clausen, M.H., Stark, R.E., and Rose, J.K.C. (2014). Tomato Cutin Deficient 1 (CD1) and putative orthologs comprise an ancient family of cutin synthase-like (CUS) proteins that are conserved among land plants. Plant J. **77**: 667–675.

Yeats, T.H., Martin, L.B.B., Viart, H.M.-F., Isaacson, T., He, Y., Zhao, L., Matas, A.J., Buda, G.J., Domozych, D.S., Clausen, M.H., and Rose, J.K.C. (2012). The identification of cutin synthase: formation of the plant polyester cutin. Nat. Chem. Biol. **8**: 609–611.

Zhai, S., Xia, X., and He, Z. (2016). Carotenoids in staple cereals: metabolism, regulation, and genetic manipulation. Front. Plant Sci. **7**: 1–13.

Zhang, B., Zhang, L., Li, F., Zhang, D., Liu, X., Wang, H., Xu, Z., Chu, C., and Zhou, Y. (2017). Control of secondary cell wall patterning involves xylan deacetylation by a GDSL esterase. Nat. Plants **3**: 17017.

Ziegler, J.U., Wahl, S., Würschum, T., Longin, C.F.H., Carle, R., and Schweiggert, R.M. (2015). Lutein and Lutein Esters in Whole Grain Flours Made from 75 Genotypes of 5 \emph{Triticum} Species Grown at Multiple Sites. J. Agric. Food Chem. **63**: 5061–5071.

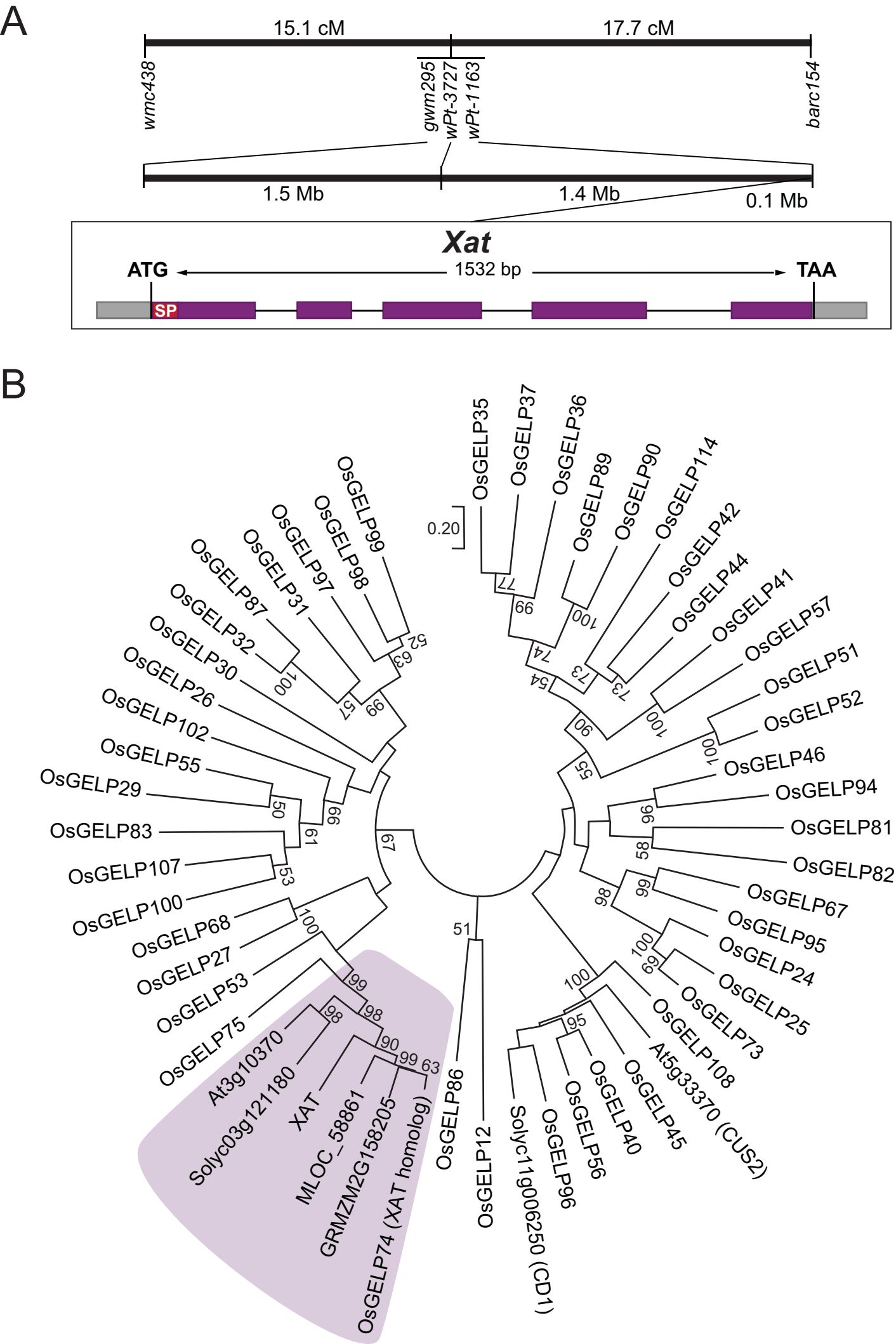
A
15.1 cM
17.7 cM
wmc438
gwm295
wPt-3727
wPt-1163
barc154
1.5 Mb
1.4 Mb
0.1 Mb
Xat
ATG
1532 bp
TAA
SP
B
0.20
OsGELP35
OsGELP37
OsGELP36
OsGELP89
OsGELP90
OsGELP114
OsGELP42
OsGELP44
OsGELP41
OsGELP57
OsGELP51
OsGELP52
OsGELP46
OsGELP94
OsGELP81
OsGELP82
OsGELP67
OsGELP95
OsGELP24
OsGELP25
OsGELP73
OsGELP108
At5g33370 (CUS2)
OsGELP45
OsGELP40
OsGELP56
OsGELP96
Solyc11g006250 (CD1)
OsGELP12
OsGELP86
OsGELP74 (XAT homolog)
GRMZM2G158205
MLOC_58861
XAT
Solyc03g121180
At3g10370
OsGELP75
OsGELP53
OsGELP27
OsGELP68
OsGELP100
OsGELP107
OsGELP83
OsGELP29
OsGELP55
OsGELP102
OsGELP26
OsGELP30
OsGELP32
OsGELP87
OsGELP31
OsGELP97
OsGELP98
OsGELP99

Figure 1. *Xat* Gene Structure and Phylogenetic Analysis with GDSL Esterase/Lipase Homologs from Rice and Various Plant Species.
(A) Mapped location of *Xat* (TraesCS7D01G094000) on chromosome 7D of bread wheat (*Triticum aestivum*) as determined previously (Ahmad *et al.* 2015). *Xat* gene structure: exons, purple boxes; untranslated regions, gray boxes; putative signal peptide (SP), red box. **(B)** Phylogenetic analysis of XAT and its homologs from various plant species. The phylogenetic tree includes XAT homologs, highlighted in purple, and related sequences, as described in Methods.

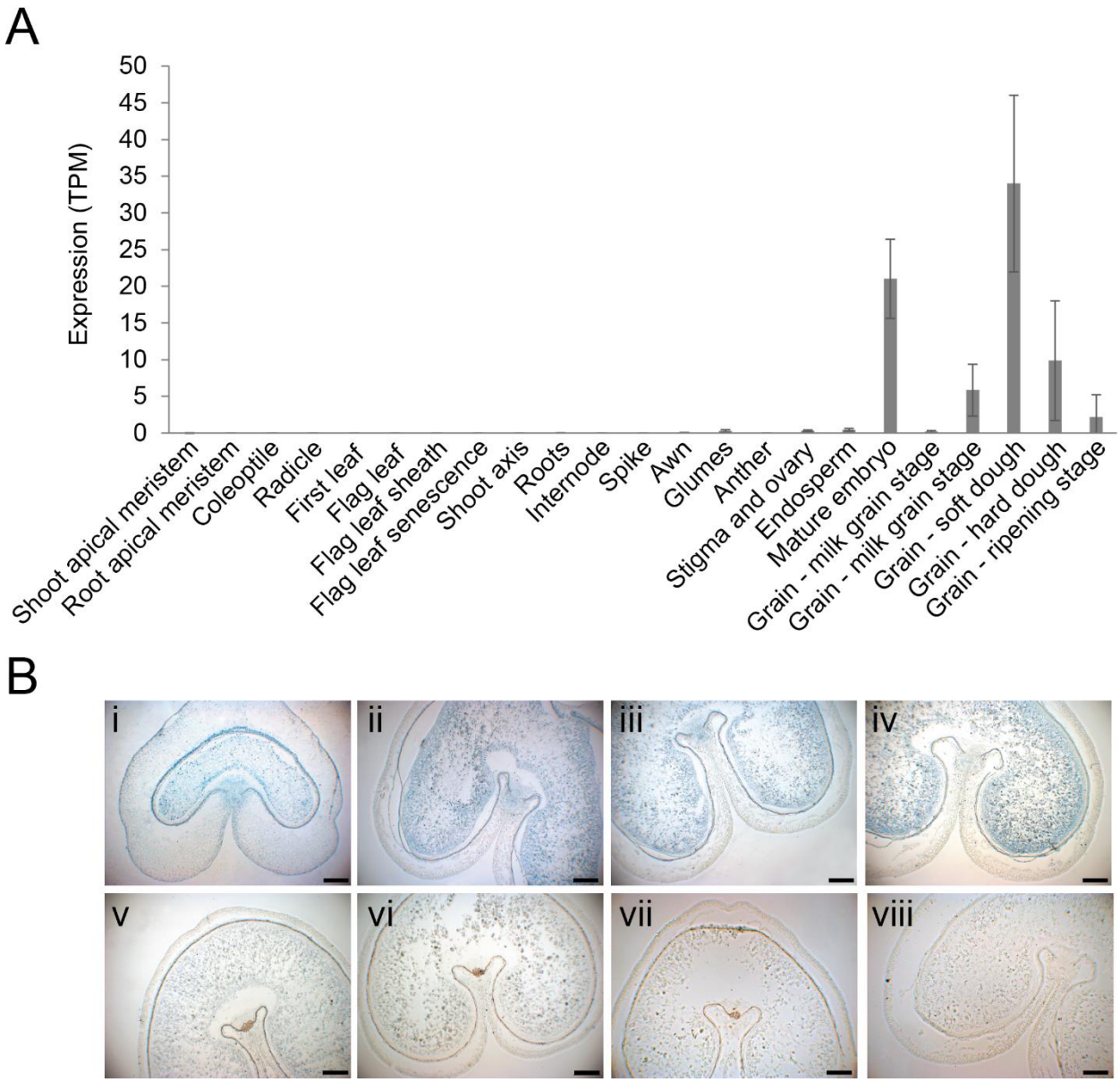

Figure 2. Spatial and Developmental Distribution of *Xat* Expression.
(A) Expression of *Xat* across different tissues and developmental stages of bread wheat (Azhurnaya cultivar). RNA-seq data were generated by Ramírez-González et al., (2018) where error bars represent ± SD for three biological replicates which consist of five individual plants sampled for tissues at each developmental stages. **(B)** Spatial expression profiles of *Xat* demonstrated via mRNA in situ hybridization using DIG-labelled riboprobes on transverse sections of developing grains from the wild type hexaploid wheat cultivar Gladius (**i-iv,** representing 7, 9-10, 12-13 and 21-22 d after pollination (DAP), respectively) and the zero-ester wheat line DM06.6*008 (**v,** 11 DAP) and the zero-ester cultivar Haruhikari (**vi,** 17 DAP). Immunological detection and color development are described in Methods. Signals observed in the zero-ester lines were similar to background signals observed in the no-antibody, no-probe controls for both Gladius (**vii,** 12-13 DAP) and Haruhikari (**viii,** 12-13 DAP). Scale bar, 400 µm.

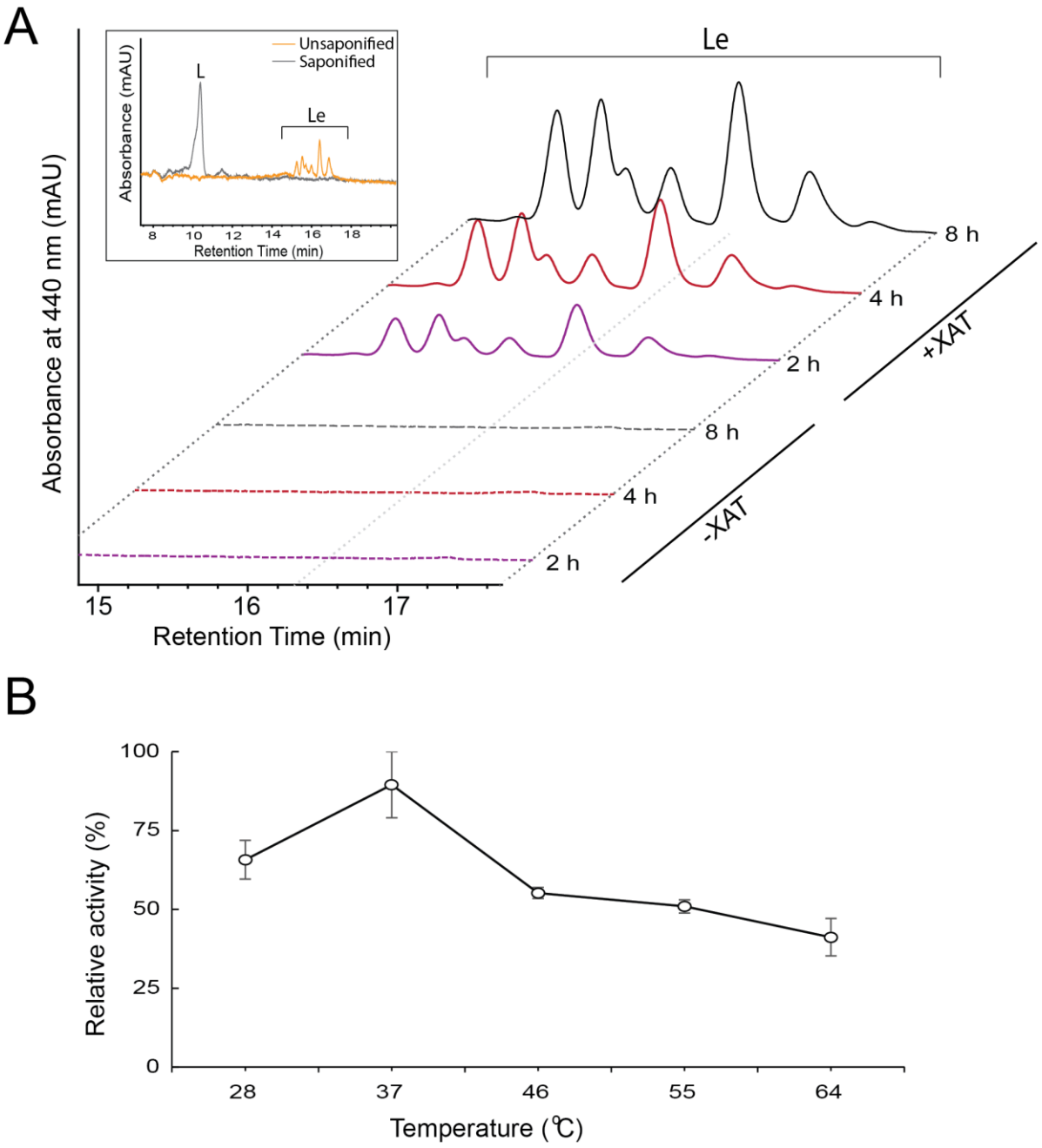

Figure 3. Recombinant XAT1 Catalyzes Formation of Xanthophyll Esters and is Active Across a Broad Temperature Range.

(A) HPLC analysis of XAT (20 µg) activity after 2, 4, and 8 h incubation at 37°C (each trace is a representative of n = 3 biological replicates. Inset, HPLC analysis after saponification performed on lutein ester fractions from the XAT enzyme assay. L, free all-*trans* lutein, Le, lutein esters **(B)** Temperature dependence of XAT activity. XAT activity (20 µg) was assayed for 4 h at 28, 37, 46, 55 and 64°C. Error bars represent ± SE for n = 3 biological replicates.

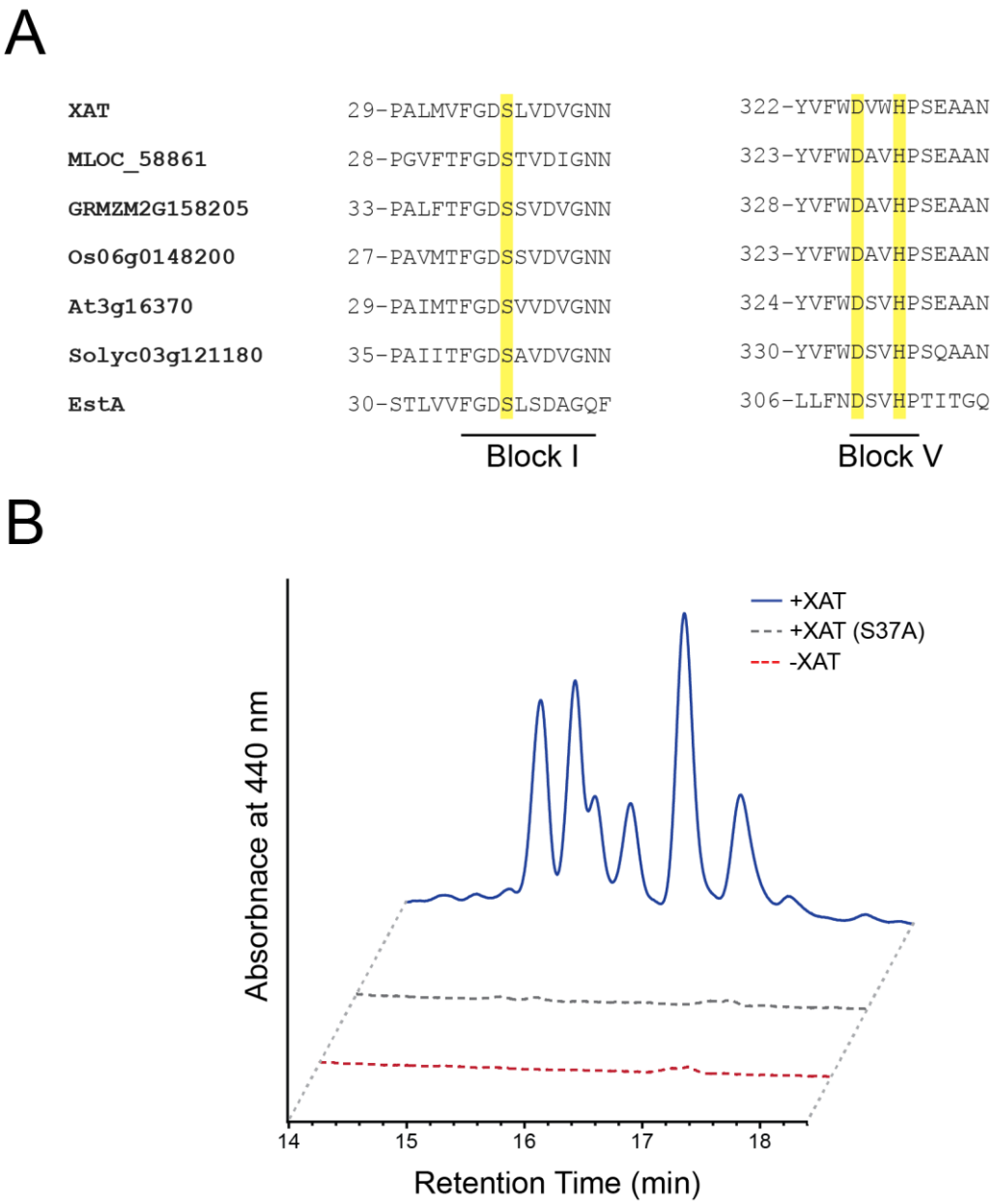

Figure 4. XAT Activity is Dependent on a Conserved Ser Residue in Block I.
(A) Alignment of XAT and homologous protein sequences from various plant species and one bacterial species. Barley (*Hordeum vulgare,* MLOC 58861), maize (*Zea mays*, GRMZM2G158205), rice (*Oryza sativa,* Os06g148200), *Arabidopsis thaliana* (At3g16370), tomato (*Solanum lycopersicum,* Solyc03g121180) and EstA from *Pseudomonas aeruginosa* (PDB accession number 3KVN). Yellow highlighted residues form the putative catalytic triad. Black lines indicate Block I and Block V homology as previously designated (Akoh *et al.* 2004). **(B)** The S37A mutation completely inhibits XAT lutein esterification activity. HPLC analysis of mutated XAT(S37A) (80 µg) activity after 4 h at 37°C and pH 8.0 compared to activity of WT XAT (20 µg) under the same conditions. Lipids extracted from the flour of the zero-ester wheat line, DM06.6*048 were used as the acyl donor. The S37A mutant had no significant activity. Each trace is representative of n = 3 biological replicates.

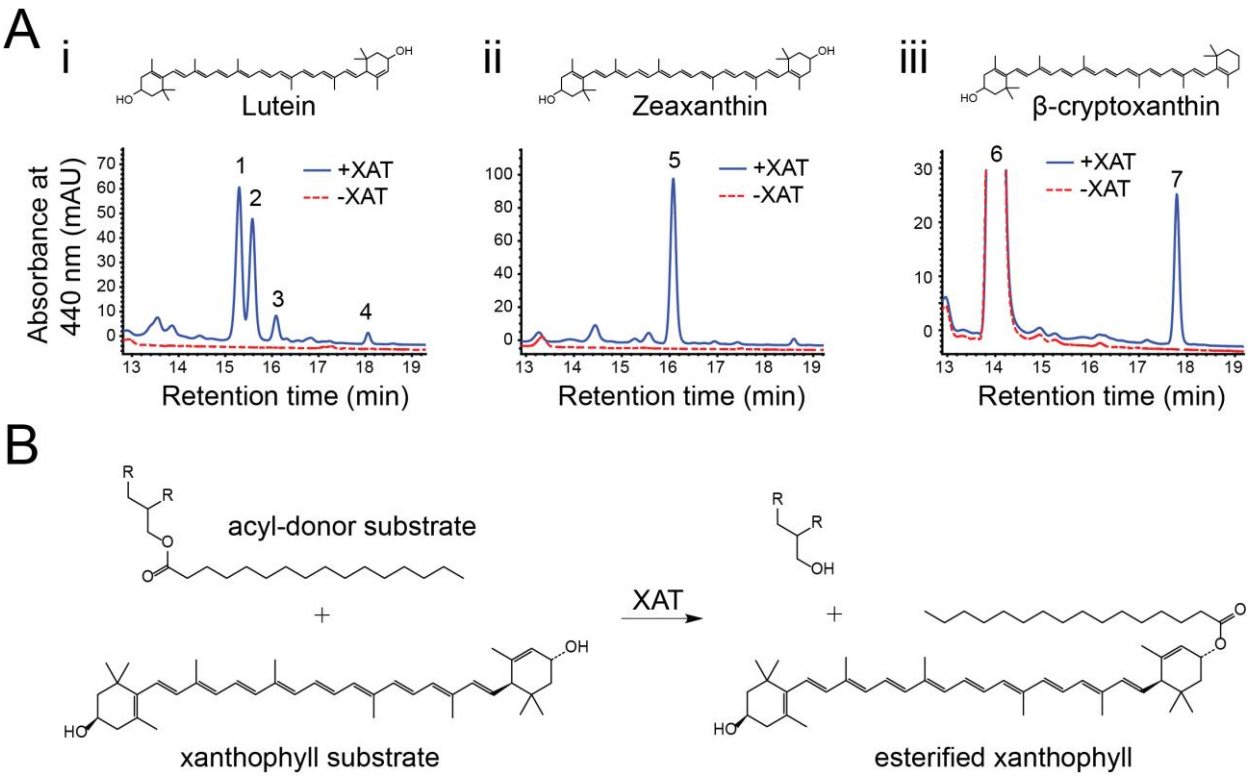

Figure 5. XAT can Esterify Multiple Xanthophyll Substrates and Functions via a Transesterification Mechanism.
(A) XAT activity (20 µg) using various xanthophyll substrates, **(i)** lutein **(ii)** zeaxanthin **(iii)** β-cryptoxanthin with 5 mM trilinolein as the acyl donor after a 4 h incubation at 37°C. Peaks 1-3, monoesters of lutein; peak 4, lutein diester; peaks 5, zeaxanthin monoester; peak 6, free *β*-cryptoxanthin; peak 7, monoester of β-cryptoxanthin. **(B)** Proposed model for esterification of xanthophylls by transesterification catalyzed by XAT. Lutein is shown as the xanthophyll acyl acceptor along with a palmitic acid lipid ester as the acyl donor.

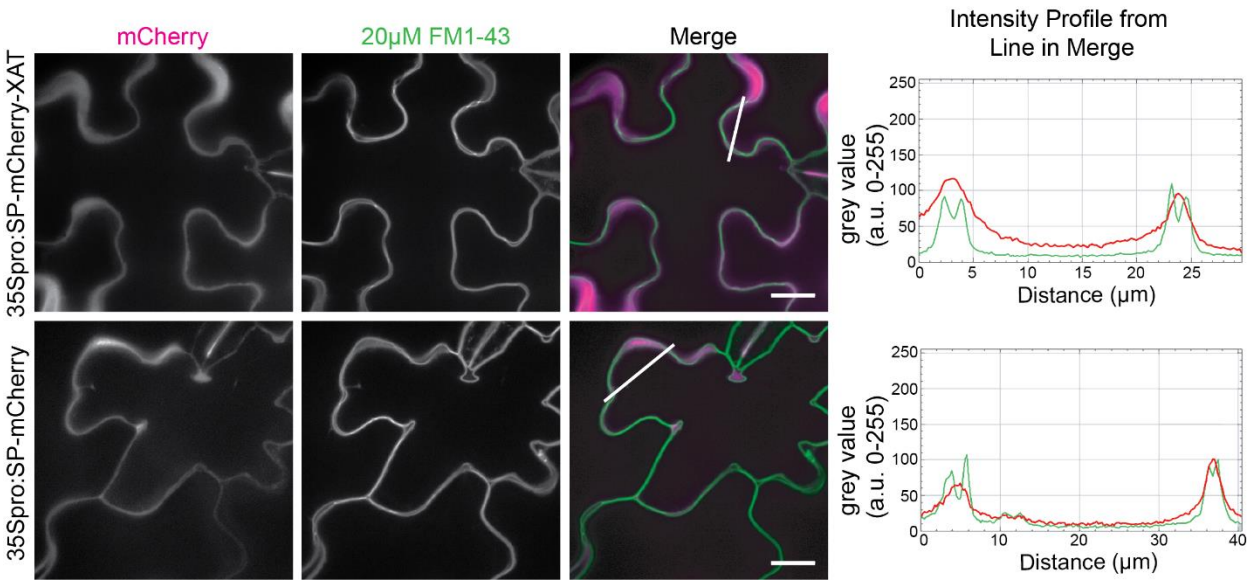

Figure 6. Localization of XAT mCherry Fusion Proteins in *N. benthamiana* Leaves.
Representative images from plants transformed with an internal fusion having either mCherry inserted between the putative signal peptide and the remainder of the coding sequence of XAT (top row) or the putative signal peptide from XAT alone fused to mCherry (bottom row). mCherry is magenta in the merged image and line scans, while counterstaining with the membrane dye, FM1-43, is green. Plots of grey values (arbitrary units, 0-255) were generated along the line indicated in the merged image to indicate the relationship between the mCherry signal and FM1-43. Grey values represent pixel intensity on a scale of 0-255. Images are single frames from *z*-stack, scale bars represent 20 µm.

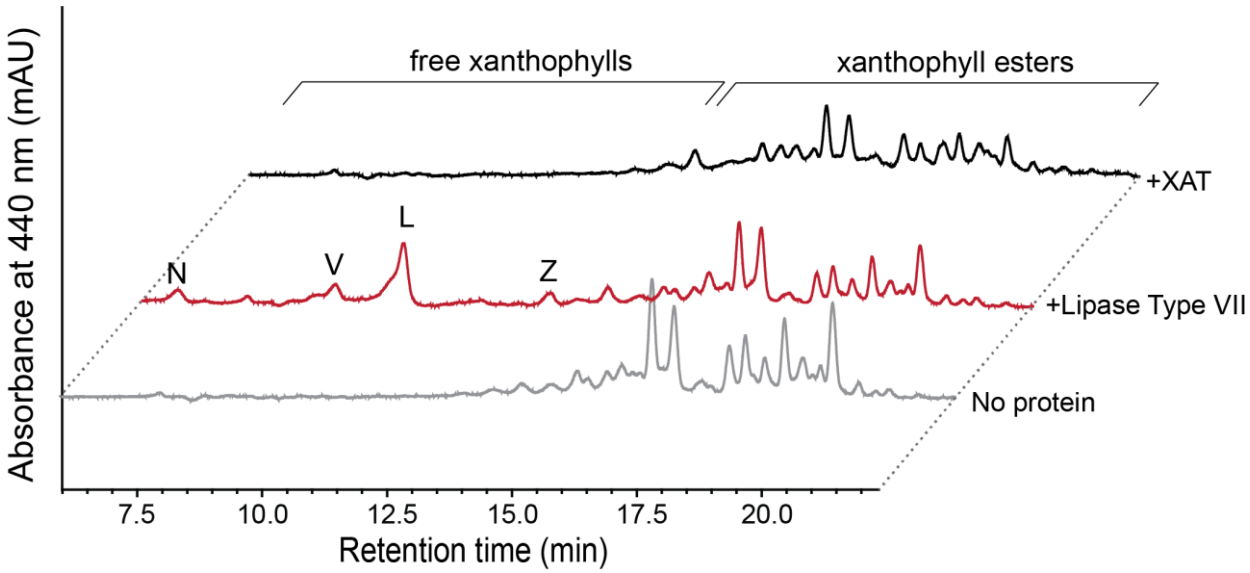

Figure 7. XAT Cannot Hydrolyze Xanthophyll Esters.
XAT (20 µg) was incubated for 4 h with lutein esters purified from marigold flowers. No free xanthophylls were released after treatment with XAT. As a control, xanthophyll esters were also incubated with lipase type VII from *Candida rugosa,* which was demonstrated to have hydrolytic activity, releasing several species of free xanthophylls as shown previously (Breithaupt *et al*. 2002). Abbreviations: L, free lutein; Z, free zeaxanthin; V, free violaxanthin; N, free neoxanthin.

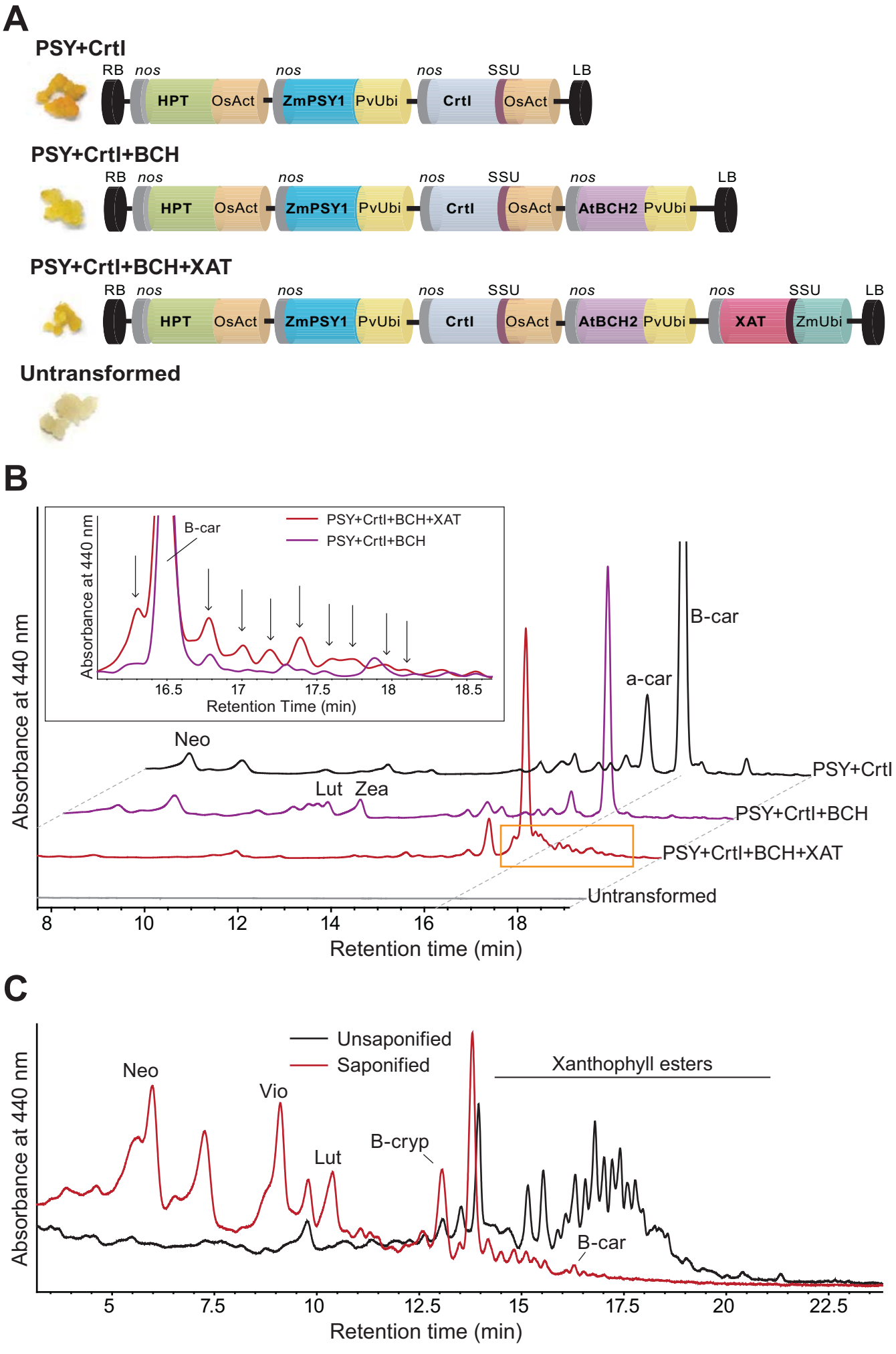
A
PSY+CrtI
RB
nos
HPT
OsAct
nos
ZmPSY1
PvUbi
nos
CrtI
SSU
OsAct
LB
PSY+CrtI+BCH
RB
nos
HPT
OsAct
nos
ZmPSY1
PvUbi
nos
CrtI
SSU
OsAct
nos
AtBCH2
PvUbi
LB
PSY+CrtI+BCH+XAT
RB
nos
HPT
OsAct
nos
ZmPSY1
PvUbi
nos
CrtI
SSU
OsAct
nos
AtBCH2
PvUbi
nos
XAT
SSU
ZmUbi
LB
Untransformed
B
Absorbance at 440 nm
B-car
PSY+CrtI+BCH+XAT
PSY+CrtI+BCH
16.5
17
17.5
18
18.5
Retention Time (min)
Neo
Lut
Zea
a-car
B-car
PSY+CrtI
PSY+CrtI+BCH
PSY+CrtI+BCH+XAT
Untransformed
Absorbance at 440 nm
8
10
12
14
16
18
Retention time (min)
C
Unsaponified
Saponified
Neo
Vio
Lut
B-cryp
Xanthophyll esters
B-car
Absorbance at 440 nm
5
7.5
10
12.5
15
17.5
20
22.5
Retention time (min)

Figure 8. Heterologous Expression of *Xat* in Carotenoid-accumulating Rice Embryogenic Callus Produces Xanthophyll Esters.
(A) Constructs generated and used to transform rice embryogenic callus. Expression of ZmPSY1 is driven by the *P. virgatum* ubiquitin promotor (PvUbi). CrtI fused with the SSU transit peptide from rubisco from *Arabidopsis* and the hygromycin resistance marker gene (HPT) are both controlled by the rice actin promotor (OsAct). *AtBCH2* is driven by the PvUbi promotor. Expression of *Xat* fused inframe to the SSU transit peptide from rubisco is controlled by the maize ubiquitin promotor (ZmUbi). Representative images of transformed lines displaying yellow to orange phenotypes are shown to the left of each construct. Untranformed callus displaying a pale phenotype is also shown. **(B)** Representative HPLC chromatograms of carotenoids extracted from each line of transformed rice callus as well as the untransformed callus as a control. Chromatograms are offset by retention time. Yellow box shows production of xanthophyll esters in a representative line which expresses *Xat* (PSY + CrtI + BCH +XAT). Inset shows production of esters in the representative line expressing *Xat* as highlighted by the yellow box and compares to the representative line expressing PSY, CrtI and BCH without XAT and without retention time offset. Arrows indicate xanthophyll esters. **(C)** HPLC analysis of carotenoids extracted from a representative transformed rice embryogenic callus line expressing *XAT* (PSY + CrtI + BCH+ XAT) after saponification treatment. Abbreviations: Lut, lutein; Zea, zeaxanthin; B-cryp, *β*-cryptoxanthin; B-car, β-carotene; Neo, neoxanthin; Vio, violaxanthin; a-car, α-carotene. Data are representative of n = 3 biological replicates. Abbreviations: RB, right border; LB, left border; nos, *nos* terminator; SSU, Arabidopsis ribulose-1,5-bisphosphate carboxylase/oxygenase small subunit.